1-1-2017

Redox Responsive Cerium Oxide Nanoparticles And Cd44 Targeted Nanomicelles For Selective Cancer Therapy

Zhaoxian Wang
Wayne State University,

REDOX RESPONSIVE CERIUM OXIDE NANOPARTICLES AND CD44 TARGETED NANOMICELLES FOR SELECTIVE CANCER THERAPY

by

ZHAOXIAN WANG

THESIS

Submitted to the Graduate School

Wayne State University

Detroit, Michigan

in partial fulfillment of the requirements

For the degree of

MASTER OF SCIENCE

2017

MAJOR: PHARMACEUTICAL SCIENCE

Approved By:

Advisor Date

ACKNOWLEDGMENTS

My deepest gratitude goes first and foremost to my advisor Dr. Arun Iyer for his constant support, encouragement, patience and guidance during my Master of Science (MS) degree program. Without his illuminating instruction and persistent help, I would not have achieved my goal. Besides my advisor, I am also greatly indebted to the rest of my thesis committee members: Dr. Fei Chen and Dr. Mohammad Mehrmohammadi, for their continuous support, motivation, constructive advice and challenging questions.

My sincere thanks also go to Dr. Fei Chen and Dr. Zhengping Yi for the assistance, encouragement and training in the basic research techniques that I learned during lab rotation. They provided all the freedom to use the equipment in their lab which helped me a lot during the Master's program.

Furthermore, many thanks go to all my lab mates in the Use-Inspired Biomaterials & Integrated Nano Delivery (U-BIND) Systems Laboratory. Special thanks to Dr. Samaresh Sau and Dr. Prashant Kesharwani for teaching me all the basic research techniques in pharmaceutics and for the encouragement and patience with me. My sincere gratitude towards Dr. Sushil Kashaw, Duy Luong, Shaimaa Yousef, Hashem Alsaab, Kaustubh Gawde, Ketki Bhise, Rami Alzhrani and Katyayani Tatiparti, for the stimulating discussions, collaborations and moral support. I really had a great deal of fun spending time in the lab with my colleagues in the last two years. Their friendship and collaboration mean a lot to me and my project would not have been successful without their support.

I would like to thank Dr. Subhash Padhye and Dr. Fazlul Sarkar for the antitumor compound CDF, Dr, Zhi Mei for TEM imaging, Dr. Asfar Azmi for fluorescent microscopy imaging and Dr. Arun Rishi for the cells lines. Finally, I am especially grateful to all the faculty and staff members of the Department of Pharmaceutical Sciences, and to all the graduate students for most critical and constant support during the past two years.

Last but not the least, I am deeply appreciative of the support given to me by my family, and my parents Aiguo Wang and Xianzhen Xu. Their love provided me inspiration and their affection and constant support was my driving force. I love you both and wish you all the happiness you ensured I had the opportunity to experience. You have all contributed irreversibly to the personality I have become. I cannot thank you enough.

TABLE OF CONTENTS

LIST OF FIGURES

aqueous solution. (B) Hydrodynamic size of SMA-TPGS-CDF nanomicelles and HA-SMA-TPGS nanomicelles by DLS. (C) The morphology of SMA-TPGS-CDF nanomicelles and HA-SMA-TPGS nanomicelles characterized by TEM. Scale bar: 500 nm.

Figure 7. *In vitro* drug release study of SMA-TPGS-CDF nanomicelles and HA-SMA-TPGS-CDF nanomicelles incubated in PBS at pH 5.5 and 7.4, 37°C, respectively. Data are presented as mean ± SD, n=3.

Figure 8. Fluorescence microscopic images of (A) MDA-MB-231, and (B) MDA-MB-468 cells after 3h incubation with Rhodamine B labeled nanomicelles and free Rhodamine B. Blue and red colors fluorescence light indicate cell nuclei and Rhodamine B, respectively.

Figure 9. 24h and 48h viability assay on MDA-MB-231 and MDA-MB-468 treated with (A) Free CDF, SMA-TPGS-CDF nanomicelles and HA-SMA-TPGS-CDF nanomicelles at various total drug concentrations. (B) HA, SMA, TPGS, SMA-TPGS copolymer, SMA-TPGS copolymer at various total drug concentrations. Data represent mean ± SD, n=6.

Figure 10. *In vitro* cytotoxicity assay observed at 24h and 48h after CD44 receptor blockade and treating of MDA-MB-231 and MDA-MB-468 with free CDF, SMA-TPGS-CDF nanomicelles and HA-SMA-TPGS-CDF nanomicelles at various total drug concentrations. Data represent mean ± SD, n=6.

Figure 11. Free CDF, SMA-TPGS-CDF nanomicelles and HA-SMA-TPGS-CDF nanomicelles with an increasing apoptosis measured by FACs using staining of

Annexin V-FITC and PI in (A) MDA-MB-231 and (B) MDA-MB-468. SMA-TPGS copolymer, SMA-TPGS copolymer set as control.

Figure 12. Western blot showing the expression downregulation of PTEN level and upregulation of NF-κB level in protein level after treating with the CDF, SMA-TPGS-CDF nanomicelles and HA-SMA-TPGS-CDF nanomicelles in (A) MDA-MB-231 and (B) MDA-MB-468 cells.

CHAPTER 1 INTRODUCTION

1.1. Background

Cancer is known as a group of diseases characterized by cellular mutation and uncontrolled growth. If the spread of the cancer cells is out of control, eventually It can cause death. It is estimated that approximately 1,700,000 of new cancer cases occurred and over 600,000 patients are expected to die of cancer in the US, which translates to more than 1,600 people per day in 2017 [1]. Most of the current treatments for cancer are surgery [2,3] which is often combined with chemotherapy [4–6], hormonal therapy [7], radiation [8] and targeted therapy [9]. Currently, chemotherapy is the first line therapy for patients after having some type of surgery for cancer [10,11]. However, the major limitations of neoadjuvant chemotherapy is the non-specific distribution in the human body which often cause unexpected side effects to normal cells [12]. Multiple drug resistance (MDR) of cancer cells is another limitation of chemotherapeutic drugs[13,14]. The severe non-target and multiple drug resistance could be overcome if drugs could be delivered to targeted site towards cancer cells. Targeted therapeutics have a great clinical potential in increasing the cytotoxicity of cancer cells and decreasing side effects to normal cells [15].

1.2. Cerium oxide nanoparticles and its anti-cancer effects by reactive oxygen species modulation

Nanotechnology using organic and inorganic materials can play a meaningful role in addressing the selective therapy of cancers. The application of nanotechnology has seen rapid growth in many areas such as, [16], nanomedicine products[17],

imaging[18] and drug delivery[19]. Different metal oxide nanoparticles, including iron oxide nanoparticles[20–22], zinc oxide nanoparticles[23], gallium oxide nanoparticles[24], have been widely investigated for their anti-cancer effects. Cerium oxide nanoparticles have the ability to undergo oxidation-reduction cycles between valence state of Ce^{+3} and Ce^{+4} which is related to redox reactions[25,26]. Cerium oxide displays a unique pH-dependent antioxidant activity. At normal pH, it shows antioxidant properties which can protect the cells by scavenging reactive oxygen species [27], whereas in acidic pH (cancer cells environment) it presents more cytotoxicity by mediating oxidative stress to the cancer cells[28]. Along these lines, redox responsive cerium oxide nanoparticles can play a versatile role in cancer therapy due to reactive oxygen species. The physicochemical characterization, cytotoxicity of cerium oxide nanoparticles and the quantification of intracellular levels of reactive oxygen species were evaluated in detail.

1.3. Targeted anticancer drug delivery using hyaluronic acid engineered nanomicelles

1.3.1 CDF (3,4-difluorobenzylidene diferuloylmethane) – highly potent but extremely lipophilic anticancer drug

In our previous study, 3,4-difluorobenzylidene diferuloylmethane or in short CDF was synthesized that showed better bioavailability than its natural analog, diferuloylmethane, in various type of cell lines, include pancreatic, breast, lung, cervical and ovarian cancers. It has several folds higher stability with better half-life compare with its natural analog, curcumin[29]. CDF can cause inactivation of carcinomas signaling pathways consistent with miR-21 down-regulation of

transcription of DNA, NF-κb, and up-regulation of MiR-200 and phosphatase and tensin homolog (PTEN)[30–32]. However, the major issue limiting CDF for preclinical and clinical translation is its highly hydrophobicity. Therefore, In our earlier studies, we successful synthesized different formulation including dendrimer, nanoparticles and liposomes to overcome CDF's solubility issue that resulted in significant increase in chemotherapeutic efficacy[12,18,33–37].

1.3.2 Hyaluronic Acid Engineered Vitamin E TPGS nanomicelles in targeted drug delivery

1.3.2.1 What are nanomicelles?

Nanomicelles are constructed using amphiphilic polymers which can self-assemble into particles with the core-shell architecture having nano-sized dimension. The inner core is composed of the hydrophobic domain which can encapsulate the hydrophobic chemotherapeutic agents, and the outer shell mostly consists of the hydrophilic group which can improve the solubility of the nanocarriers and protect the chemotherapeutic drugs from premature degradation[38–41]. The nano-range of the micelles helps the formulation effectively to target tumor through the enhanced permeability and retention (EPR-) effect[42,43]. The hydrophilic part of amphiphilic polymers can be modified with different targeting ligand such as folic acid[44,45], hyaluronic acid[34], and transferrin[46–48] to achieve active targeting. In recent years, nanomicelles have received growing scientific attention due to their effectiveness in safety and efficacy for cancer therapy. Currently, several polymeric nanomicelles-based formulations have been moved into clinical trials including Genexol-

PM[49,50]NK105[51,52], SP1049[53,54], Docetaxel-loaded targeted polymeric nanoparticles (DTXL-TNP)[55].

1.3.2.2 Tumor passive targeting strategy of nanomicelles

Targeted nano-sized chemotherapeutic strategies are generally classified into passive targeting and active targeting. Tumor tissue has a unique property to increase the accumulation of small size nanoparticles (<200nm) caused by the enhanced permeability and retention effect (EPR) which was discovered by Maeda [56–58]. The EPR effect is caused by the difference in anatomical architecture, like blood vessels, between tumor tissues and normal tissues. Tumor blood vessels secret massive vascular permeability mediators to dilate the blood vessels. The morphology and functional defectiveness of these blood vessels lead to the massive leakage of blood components such as macromolecules and nanomicelles into tumor tissue[59–61]. Moreover, nano-sized micelles can be eliminated more rapidly from healthy organs than from tumor environment via lymphatic drainage. Therefore, nanomicelles with typical size range less than 200nm are beneficial to implement passive targeting.

1.3.2.3 Tumor active targeting strategy of nanomicelles using hyaluronic acid

Hyaluronic acid (HA) is an endogenous linear anionic polysaccharide which plays significant roles in biological functions, such as maintaining cell integrity, extracellular matrix organization, promoting cell motility and angiogenesis [62–64]. It is a natural, biodegradable, non-immunogenic and biocompatible polymer, and owing to its affinity to specifically recognize overexpressed CD44 receptor. CD44

is a type 1 transmembrane glycoprotein found on hematopoietic cells, fibroblasts, and numerous tumor cells. Compared to normal cells, CD44 has higher expression on the surface of many different types of carcinomas including triple negative breast cancer [65–68]. Multiple investigators have modified HA with the carrier as an ideal biomaterial for drug delivery cancer therapy [69–71]. Active targeting drug carriers can overcome the limitation of the passive targeting approach resulting in the high accumulation of the drugs in the tumor site and less cytotoxicity to normal cells. Passive targeting can only work in highly permeable solid tumors [15]. Therefore, the efficacy of chemotherapeutics can be addressed based on modifying an active targeting ligand, such as monoclonal antibodies [72,73], peptide ligands[74–76] and small molecules [77,78], which can enhance the cellular affinity of tumor cells due to highly expressed specific receptors on the tumor cell surface. Many studies have shown the ability of nanovehicles such as nanoparticles [79], nanomicelles [34], liposomes [80] and dendrimers [12,18,36] , to deliver chemotherapeutic drugs.

1.3.2.4 Styrene-Maleic Acid (SMA) Copolymer with D-α-Tocopherol polyethylene glycol 1000 succinate (Vitamin E TPGS)

Previous studies have shown that SMA micelles exhibited a high drug loading and encapsulation efficiency, and could solve the poor aqueous solubility issue of many anticancer compounds. The SMA polymer conjugate with anticancer compound (SMANCS) has been approved for human clinical use[81,82]. D-α-Tocopherol polyethylene glycol 1000 succinate (Vitamin E TPGS) is a derivative of the natural vitamin E (PEGylated vitamin E), and has been approved by the

United State Food and Drug Administration (FDA) as well as the European Food Safety Authority (EFSA) as a safe pharmaceutical adjuvant in drug formulations [83,84]. TPGS is a P-glycoprotein inhibitor, which can inhibit the function of the efflux pump to overcome the multidrug resistance (MDR) in cancer cells [85–87]. Meanwhile, TPGS can enhance solubility, absorption, permeation and improve cellular uptake of the chemotherapeutics agents, making it a promising strategy for drug delivery system [88–90].

The aim of this study is to build up the hyaluronic acid decorated nanomicelles to achieve active targeting to CD44 receptor which is overexpressed on cancer cells (scheme 1.) We have studied the ability to form micelles of SMA-TPGS copolymer and its ability to target cancer cells by passive targeting and active targeting using HA as targeting ligand[91,92]. The resulting conjugate (HA-SMA-TPGS) can self-assemble into nanomicelles and encapsulate the hydrophobic drug CDF. The physicochemical characterization, *in vitro* cellular uptake and cytotoxicity of micelles were evaluated in detail.

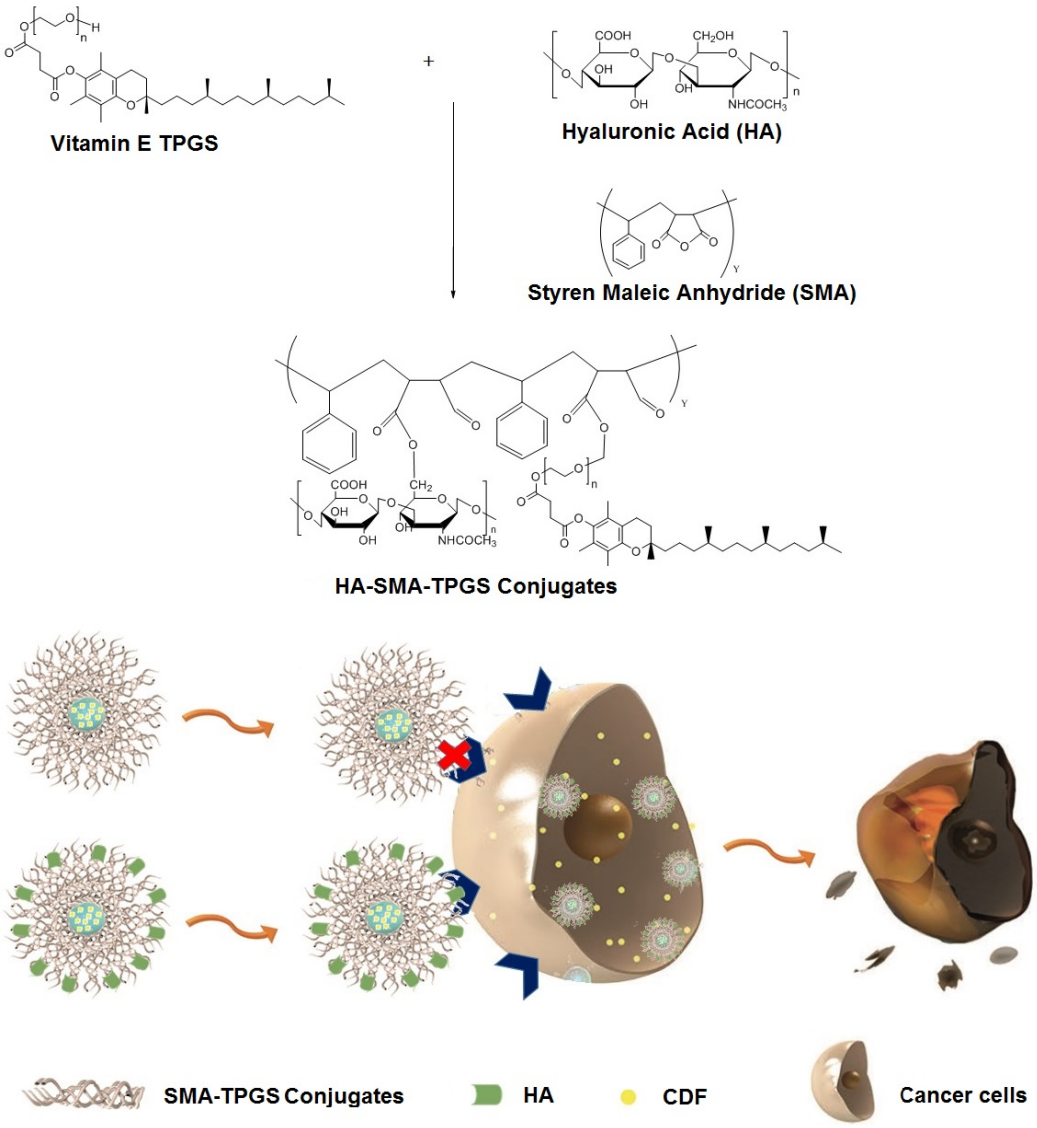

Scheme 1. Schematic illustration of synthesis HA-SMA-TPGS conjugate and self-assembly of SMA-TPGS-CDF and HA-SMA-TPGS-CDF to form nanomicelles in overexpressed CD44 receptor cancer cells.

CHAPTER 2. EXPERIMENTAL DESIGN

2.1. Materials

2.1.1 Reagent

CDF was synthesized as described early. Poly-(styrene-co-maleic anhydride), SMA (M=1.6 kDa), N-(3-(dimethylamino) propyl)-N'-ethylcarbodiimide hydrochloride (EDC), 3- [4,5 dimethylthiazol-2-yl]-2,5 diphenyltetrazolium bromide (MTT), 2',7' – Dichlorofluorescin diacetate (H2DCFDA), and Sodium bicarbonate were purchased from Sigma-Aldrich (St. Louis, MO). Hyaluronic acid (MW = 13 kDa) was purchased from Lifecore Biomedical (Chaska, MN). D-α-Tocopherol polyethylene glycol 1000 succinate (Vitamin E TPGS) was purchased from Antares health products, INC. All the other reagents used were of analytical grade and used without any modification.

2.1.2 Cells line

The human lung adenocarcinoma cell line A549 (non-small cell lung cancer) was used for our study which is based on the earlier reports of its sensitivity to cerium oxide nanoparticles. The cells lines were maintained in Kaighn's Modification of Ham's F-12 Medium (F-12K Medium, Thermo Fisher Scientific, USA) supplemented with 10%(v/v) Fatal Bovine Serum (FBS, Thermo Fisher Scientific, USA), penicillin (100 units/Ml) and streptomycin (100µg/Ml) as standard culture conditions. The human breast epithelial cell line MCF10A were cultured in Mammary Epithelial Basal Medium (MEBM™, Lonza Walkersville, Inc) supplemented with 100 ng/ml cholera toxin (Sigma-Aldrich, USA), BPE 2.0ml, Hegf 0.5ml, Insulin 0.5ml and Hydrocortisone 0.5ml (MEGM SingleQuots, Lonza

Walkersville, Inc). Human breast cell lines MDA-MB-231 and MDA-MB-468 were used as the *in vitro* model due to its overexpression of CD44 receptor (Human TNBC cell lines MDA-MB-468 and MDA-MB-231 were given by Dr. Arun Rishi from Karmanos Cancer Institute and John D. Dingell VA Medical Center, Wayne State University, Detroit, MI, USA.) All cell lines were cultured in DMEM medium with 10 % fetal bovine serum (FBS) and 1 % penicillin-streptomycin. All the cells line flasks were placed in a 37 °C incubator with 5% CO2 levels (Forma Steri-Cult HEPAClass100 CO2 incubator, Thermo Scientific).

2.2. Explore the pH-dependent redox activity in Cerium oxide nanoparticles for selective cancer cell killing

2.2.1 Characterization of cerium oxide nanoparticles

The CNPs, PEG-CNPs, GLY-CNPs, were characterized for size and zeta potential using a Beckman Coulter Delsa Nano C DLS (Beckman Coulter, Inc., Fullerton, CA) Particle analyzer equipped with a 658 nm He−Ne laser. The morphologies of three different batches of cerium oxide nanoparticles were assessed using transmission electron microscopy (TEM) (JEM 2010, Tokyo, Japan) at an accelerating voltage of 200 Kv and 100,000 X magnification.

2.2.2 Cell viability analysis by MTT assay

In vitro cytotoxicity of free cerium oxide nanoparticles and polymer-coated cerium oxide nanoparticles was determined using a 3-[4,5-dimethylthiazol-2-yl]-2, 5-diphenyltetrazolium bromide (MTT) assay. A549 cells and MCF10A cells were seeded in 96-well plates (3000 cells each well), respectively and incubated for 24h. The cells were treated with different concentration from 0.00001mg to 0.1 mg of

CNPs, PEG-CNPs, GLY-CNPs. After 24h, the cells were incubated with MTT at 37 °C with 5 % CO2 for 3h. Then the medium was discarded and replaced with by 100ml DMSO in each well. The absorbance was read at 590nm using a high-detection multi-plate reader (Synergy 2, BioTek). Percent of cell viability was calculated as (OD of sample group / OD of the control group) × 100.

2.2.3 Quantification of intracellular levels of reactive oxygen species (ROS)

The reactive oxygen species (ROS: H_2O_2) were quantified by fluorescence spectrum using F-2500/F-4500 Fluorescence Spectrophotometer Instruction. Briefly, A549 cells (2 x 10^5 cell/ml) were seeded in 6-well plates incubated for 24h. The cells were treated with 0.02mg/ml of different formulation of CeO_2 sample. After 24h, the cells were washed with PBS and treated with 30Mm H2DCFDA in cells incubator. After half hour treatment, A549 cells were detached by scraping and washed again with PBS; then cells were centrifuged to obtain the pellet. The pellet was lysed using lysis buffer with protease inhibitor cocktail. Bradford assay was performed to detect the protein concentration. Cell lysate was used to determine the fluorescence intensity in fluorescence spectrum. The quantification of intracellular levels of ROS was evaluated as fluorescence intensity of same concentration of protein.

2.3. Hyaluronic acid engineered nanomicelles (HA-SMA-TPGS) for the targeted delivery of CDF to CD44 overexpressing cancer cells

2.3.1 Synthesis and Characterization of SMA-TPGS Conjugates (Non-targeted) and HA-SMA-TPGS Conjugates (Targeted)

For the synthesis of the targeted and non-targeted conjugates, a known ratio of HA and TPGS was mixed well in deionized water (DI water) at RT, and 1M $NaHCO_3$ was added to the solution slowly and stirred for several hours. Then the pH was raised to 8.9 and Poly- (styrene-co-maleic anhydride) (SMA) was added dropwise to the HA and TPGS solution under magnetic stirring. After that, the reaction was done until the solution became clear. Only difference in non-targeted conjugates is, at beginning HA was not added into the solution. SMA-TPGS conjugates and HA-SMA-TPGS conjugates were purified by dialysis bag (MW 2 kDa) for 24 h and the solution was lyophilized and characterization by proton nuclear magnetic resonance spectroscopy (^{1}H NMR) and Fourier transform infrared spectroscopy (FTIR). The critical micelle concentration (CMC) of SMA-TPGS and HA-SMA-TPGS was determined by a pyrene fluorescence method. In briefly, 100 µL of pyrene solution (12 µM in methanol) added into amber color bottle, and the methanol was evaporated under shaking overnight at room temperature. 2 ml of the sample solution with a series of concentrations was added into each amber bottle. The fluorescence spectrum was recorded using F-2500/F-4500 Fluorescence Spectrophotometer Instruction. The CMC value is determined by plotting the fluorescence intensity of excitation wavelengths ratio ($I_{335\ nm}$/ $I_{332\ nm}$) as a function of polymer concentration.

2.3.2 Preparation and Characterization of CDF – loaded Nanomicelles

SMA-TPGS-CDF and HA-SMA-TPGS-CDF were prepared according to our previous reported method[34,93]. First, 100 mg of conjugates polymer was dissolved in 100 ml of DI water under stirring. Then CDF (30 mg) were dissolved in 1 ml of DMSO and mixed with the polymer solution. After that 40 mg of EDC was added dropwise into solution and pH was kept at 5.0 to stir for 30 min. Then raised pH to 11 and kept for other 30 min. At last, pH was adjusted to 7.8 – 8.0 and the free drug CDF were removed by dialysis bag for 4 – 5 hours (MW 2 kDa). Eventually, the solution was lyophilized to obtain the final nanomicelles. Average particle size of CDF – loaded nanomicelles were measured using Dynamic Light Scattering (DLS, Beckman Coulter Delsa Nano CTM). In addition, the size distribution and morphology was observed by transmission electron microscopy (TEM, H-7500, and Hitachi Ltd, Tokyo, Japan).

2.3.3 Drug Encapsulation and Loading

The encapsulation efficiency and drug loading content of CDF-loaded nanomicelles were determined by high-performance liquid chromatography (HPLC) analysis. The lyophilized nanomicelles were dissolved in deionized water and subjected to sonication for removal of encapsulated drug. Then the sample was quantitatively analyzed by HPLC. The mobile phase consisted of 70% methanol, 29.55% water and 0.45% formic acid (v/v/v) with 1 ml/min flow rate. The injection volume was 10μL and it was replicated three times. The UV detection wavelength in HPLC were set at 447 nm. The encapsulation efficiency and durg loading efficiency were calculated by the following equations:

$$Encapsulation\ efficiency\ (\%) = \frac{Amount\ of\ CDF\ in\ micelles}{Amount\ of\ CDF\ used} \times 100$$

$$Durg\ Loading\ efficiency\ (\%) = \frac{Amount\ of\ CDF\ in\ micelles}{Amount\ of\ micelles} \times 100$$

2.3.4 *In vitro* Release Profile of CDF-Loaded Nanomicelles

The release of CDF from the SMA-TPGS and HA-SMA-TPGS micelles was determined in phosphate buffer solution (PBS, PH 7.4). Briefly, SMA-TPGS-CDF and HA-SMA-TPGS-CDF (1 mg of CDF) were placed in 5 ml PBS (pH 5.5 or 7.4) containing 0.5% (w/w) Tween-80 in a dialysis bag (MWCO = 2K) and incubated in 20ml of PBS corresponding solution with gentle agitation at 37°C in the dark. The PBS solution outside the dialysis solution was collected at designated time (1 h, 3 h, 6 h, 9 h, 12 h, 24 h, 36 h, 48 h, and 72 h) and an equivalent volume of fresh PBS was compensated. The collected PBS solution was determined by HPLC analysis.

2.3.5 Cellular Uptake Study

In-vitro cellular uptake study was done using both CD44 overexpressed cells line, MDA-MB-231 and MDA-MB-468. First, 2×10^5 cells MDA-MB-231 and MDA-MB-468 cells were seeded in24-well plate. After 24h, the medium was removed and the cells were treated with Rhodamine B labeled formulations (SMA-TPGS-Rho and HA-SMA-TPGS-Rho) diluted with serum free DMEM medium for 3 h. Then all of the medium was removed and the cells were washed three times with PBS containing 0.1% FBS and fixed with 4% formaldehyde at room temperature for 15 min. After washing another three times, the nuclei were stained

with Hoechst 33342 (10 μg/ml) for 15 min. After washing again, the cellular uptake was studied using two fluorescence channels: blue for the Hoechst 33342 and red for the Rhodamine B.

2.3.6 *In vitro* Cytotoxicity Assay

The cytotoxicity of SMA-TPGS conjugates, HA-SMA-TPGS conjugates, free CDF, targeted and non-targeted CDF micelles was evaluated by MTT assay. MDA-MBA-231 and MDA-MB-468 cells were seeded 3000 cells each well in 96-well plate with 100 μL of full medium DMEM (10% FBS and 1% antibiotics) and incubated at 37°C in humidified environment of 5% CO_2 overnight to allow cell attachment. After that, the medium was removed, and different concentrations of conjugates and CDF micelles were diluted with fresh medium and added into the cells. After 24 h and 48 h, the medium was removed and 100 μL of 1 mg/ml MTT in PBS was added to each well. The plates were put back to the incubator for other 4 h. Then removed MTT add 100 μl of DMSO was added to the plates. After gentle shaking, the absorbance was measured at 595 nm by plate reader. The results were calculated as the mean percentages of the viability of treated cells relative to untreated cells. The cell viability was evaluated through the equation:

$$Cell\ viability\ (\%) = \frac{Absorbance\ of\ treated\ cells}{Absorbance\ of\ untreated\ cells} \times 100$$

2.3.7 CD44 Receptor Blocking Assay

The CD44 receptor blockade assay based on the principle of occupying the CD44 receptor using an excess amount of HA (5 mg/ml), After the CD44 receptor were blocked, and the cells were treated with different concentrations of

formulations. The cell viability was evaluated by MTT assay again as described above.

2.3.8 Flow Cytometry Analysis

MDA-MB-231 and MDA-MB-468 cells (2×10^5 cells/well) were seeded in 6-well plate for overnight at the incubator. After that, free SMA-TPGS conjugated, HA-SMA-TPGS conjugated, free CDF, SMA-TPGS-CDF and HA-SMA-TPGS-CDF were added in FBS-containing-DMEM medium to treat the cells. After the cells had been incubated for 12 hours, cells were trypsinized and analyzed by apoptosis assay using Guava Nexin Annexin V assay (EMD Millipore, USA) as described by the manufacturer. Briefly, the cells were collected with the media to centrifuge. The pellets were dispersed in PBS containing 1% Fetal Bovine Serum. Then 150μL of cell dispersion was mixed with 50μL of the Guava Nexin Reagent and kept in the dark for 10 minutes. The sample was studied for early and late apoptosis by Guava Easycyte flow cytometer.

2.3.9 Western Blot

The cells were collected with PBS and lysed with lysis buffer. Total protein content was performed using Bradford assay. An equal amount of protein (30 mg) was separated by 10% SDS-PAGE and transferred to a nitrocellulose membrane. For detection of specific protein, nitrocellulose membrane was incubated with PTEN and NF-κb after blocking in 5% nonfat milk solution. (PTEN, NF-κb antibodies were purchased from Cell Signaling Technology, USA). HRP-linker rabbit secondary antibodies were used to detect the immunoreactions and the Blots was exposed by X-ray film.

CHAPTER 3. RESULTS

3.1. Explore the pH-dependent redox activity in Cerium oxide nanoparticles for selective cancer cell killing

3.1.1. Characterization of cerium oxide nanoparticles

The cerium oxide nanoparticles were bought from US Research Nanomaterial, Inc with the size is 10nm. The TEM image shown below indicates that the size of cerium oxide nanoparticles is approximately 15 nm. (Figure 1.)

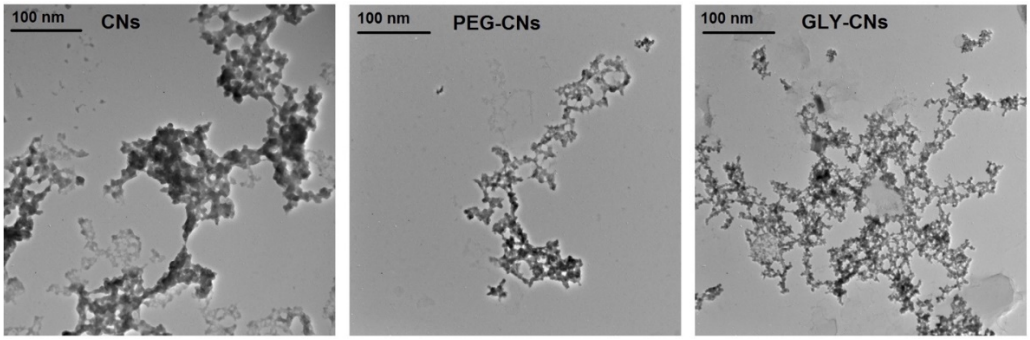

Figure 1. Transmission electron microscopy(TEM) image of CNs, PEG-CNs and GLY-CNs. Scale bar: 100 nm.

3.1.2. Cell viability analysis by MTT assay

The cytotoxicity results in Figure 2 indicated that both CNPs, PEG-CNPs and GLY-CNPs demonstrated more cytotoxicity towards A549 cancer cells in low pH (pH 6.5, generally is tumor environment) compared to normal physiological pH (pH 7.4, generally is normal tissue environment). However, lower concentration shows a higher cytotoxicity, which is probably because of the solubility issue of cerium oxide nanoparticles. The higher concentration of cerium oxide nanoparticles, the less cerium oxide nanoparticles could be dissolved in aqueous media. Both the CNPs, PEG-CNPs and GLY-CNPs showed less cytotoxicity in

normal physiological pH (pH 7.4, generally is normal tissue environment). The main reason for this bifunctional mode of action is because of the ability of pH - dependent redox activity in cerium oxide nanoparticles that can be exploited for selective cancer cell killing.

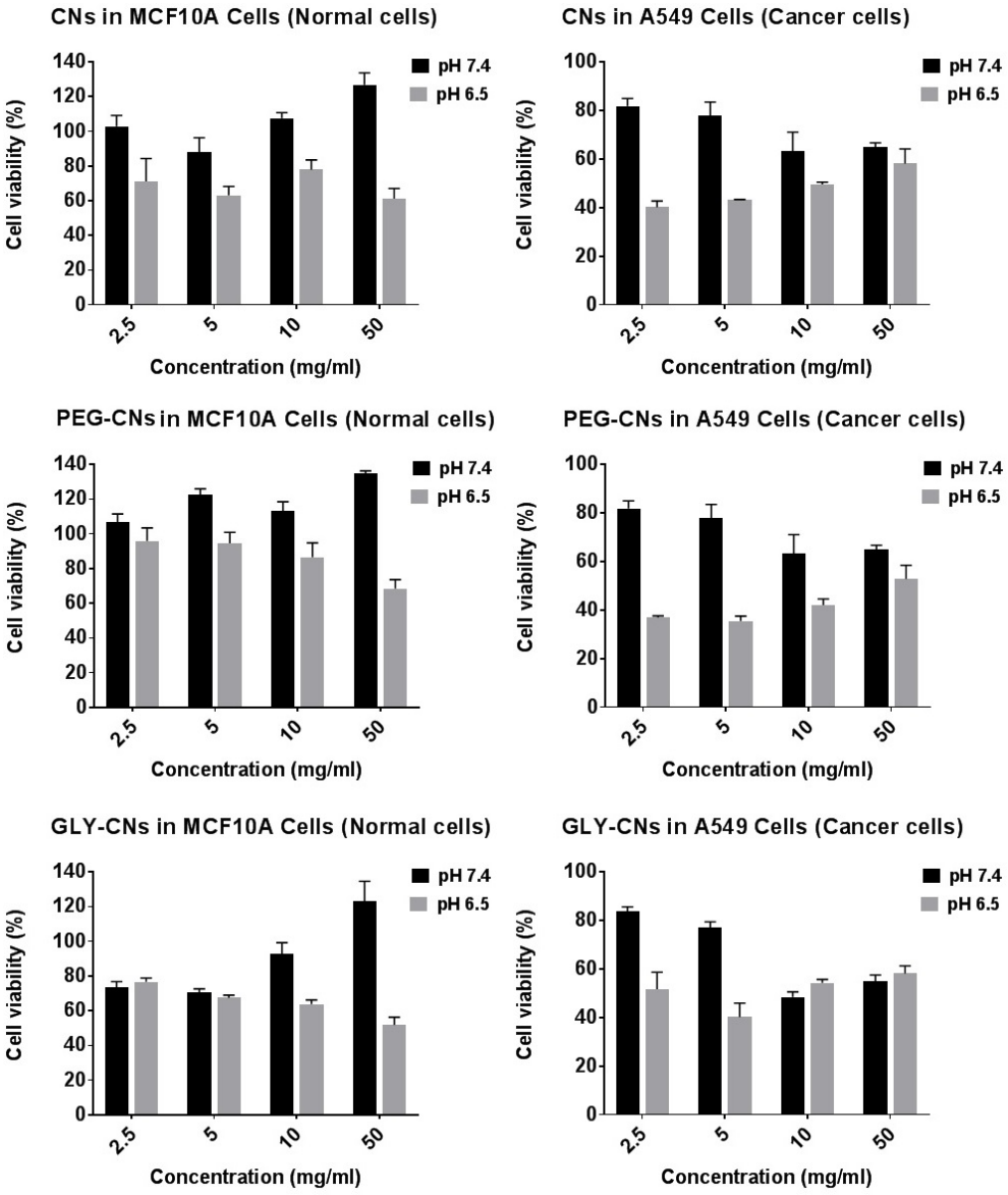

Figure 2. *In vitro* cell viability assay showing % live cells at 24h after treating MCF10A (normal breast cells) and A549 (lung cancer cells) with NPs at pH 6.5 and 7.4 at various concentrations. Data represent mean ± SD, n=5.

3.1.3. Quantification of intracellular levels of reactive oxygen species (ROS)

The relative fluorescence intensity indicates the intracellular level of ROS. As shown in figure 3, both treatments of CNPs, PEG-CNPs and GLY-CNPs clearly present significantly more ROS compared to untreated control cells. It can be concluded that the production and elevation of ROS is one of the mechanisms of anti-tumor activity of cerium oxide under low pH conditions.

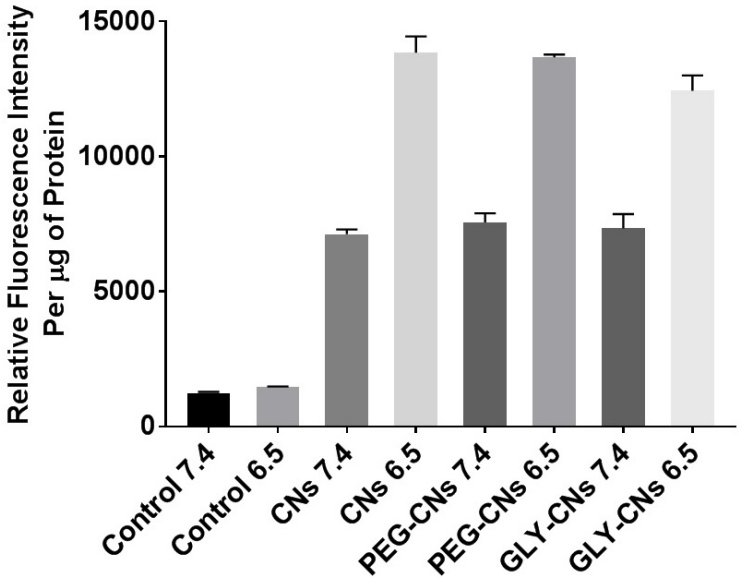

Figure 3. Quantification of intracellular ROS (H_2O_2) in A549 cells at pH 6.5 and 7.4. The results show all the treatments CNs, PEG-CNs and GLY-CNs at pH 6.5 produce more intracellular ROS (H_2O_2) compare to pH 7.4 and untreated control experiment. Data represent mean ± SD, n=3.

3.2. Hyaluronic acid engineered nanomicelles (HA-SMA-TPGS) for the targeted delivery of CDF to CD44 overexpressing cancer cells

3.2.1 Synthesis and Characterization of TPGS-SMA Conjugates (Non-targeted) and HA-TPGS-SMA Conjugates (Targeted)

The chemical structure of TPGS-SMA conjugates and HA-TPGS-SMA conjugates was confirmed using ^{1}H NMR and FTIR spectroscopy, as shown in

figure 5. As showed in the spectrum, the characterized peak of HA appeared at 3.2 – 4.1 ppm (glucosidic H), 4.4 – 4.6 ppm (anomeric H) and SMA appeared at 6.5 – 7.5 ppm, 2.5 ppm and TPGS appeared around 2.0 ppm, 4.0 ppm. Retention of characteristic peaks in TPGS-SMA conjugated and HA-TPGS-SMA confirmed the conjugates were successfully synthesized. Furthermore, FTIR spectra in figure 4 of the targeted and non-targeted conjugates showed stretching vibration peak of the ester group (-- C = O --) of conjugates at 1735 cm^{-1}, also indicating the formation of TPGS-SMA and HA-TPGS-SMA conjugate.

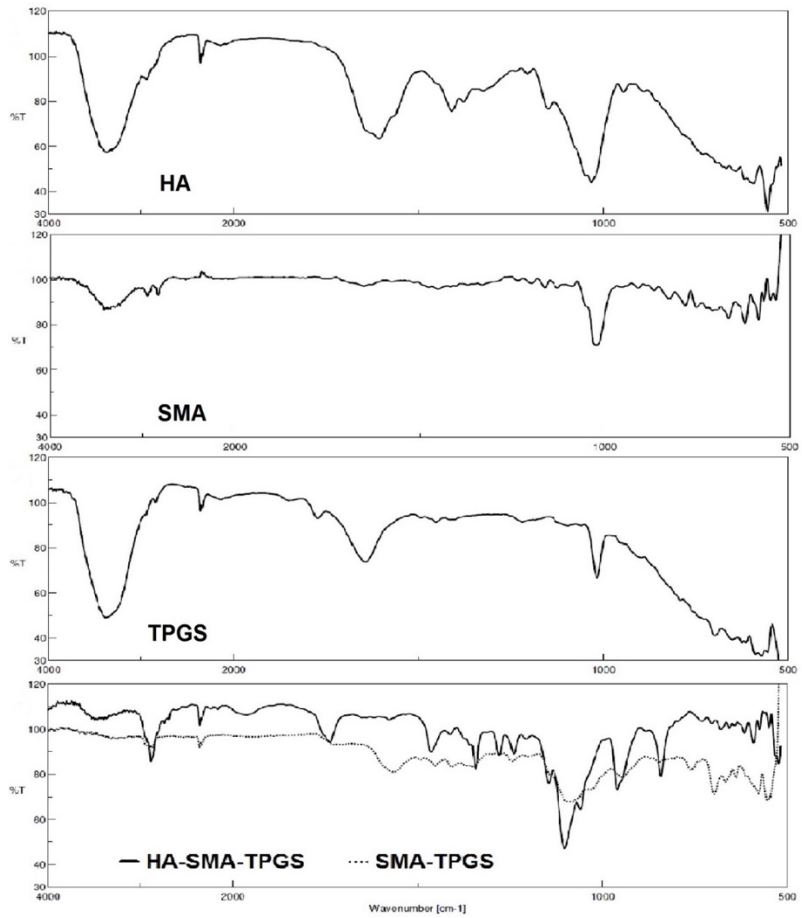

Figure 4. Fourier transform infrared spectroscopy (FTIR) of native HA, SMA polymer, TPGS and SMA-TPGS conjugates, HA-SMA-TPGS conjugates are shown.

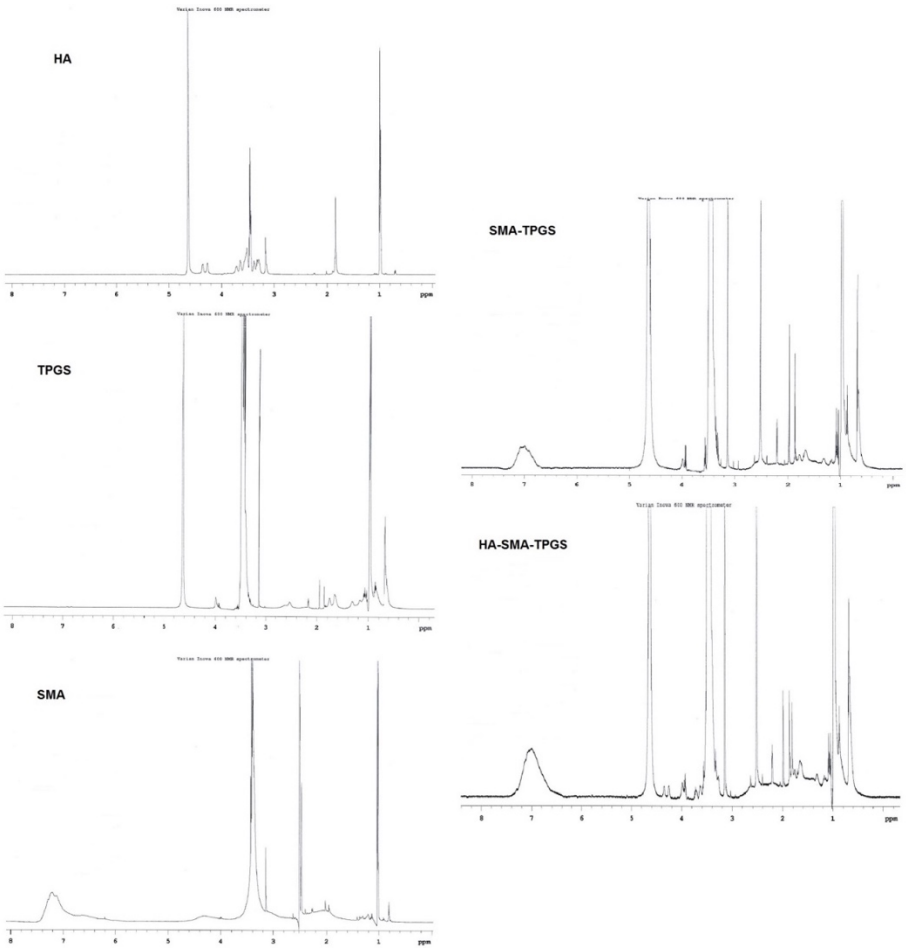

Figure 5. Characterization of HA, SMA, TPGS and SMA-TPGS conjugates and HA-SMA-TPGS conjugates by proton nuclear magnetic resonance spectroscopy (^{1}H NMR).

The conjugates in an aqueous phase could self-assemble into micelles owing to the hydrophobic part in SMA and TPGS. In figure 6A the plotting of fluorescence intensity of excitation wavelengths ratio (I_{335}/ I_{332}) increase from 0.87 to 1.14 with increasing concentration of conjugates. The CMC of both conjugates is less than 0.001 mg/ml which indicate a strong tendency of conjugates towards formation of nanomicelles in water at a lower concentration.

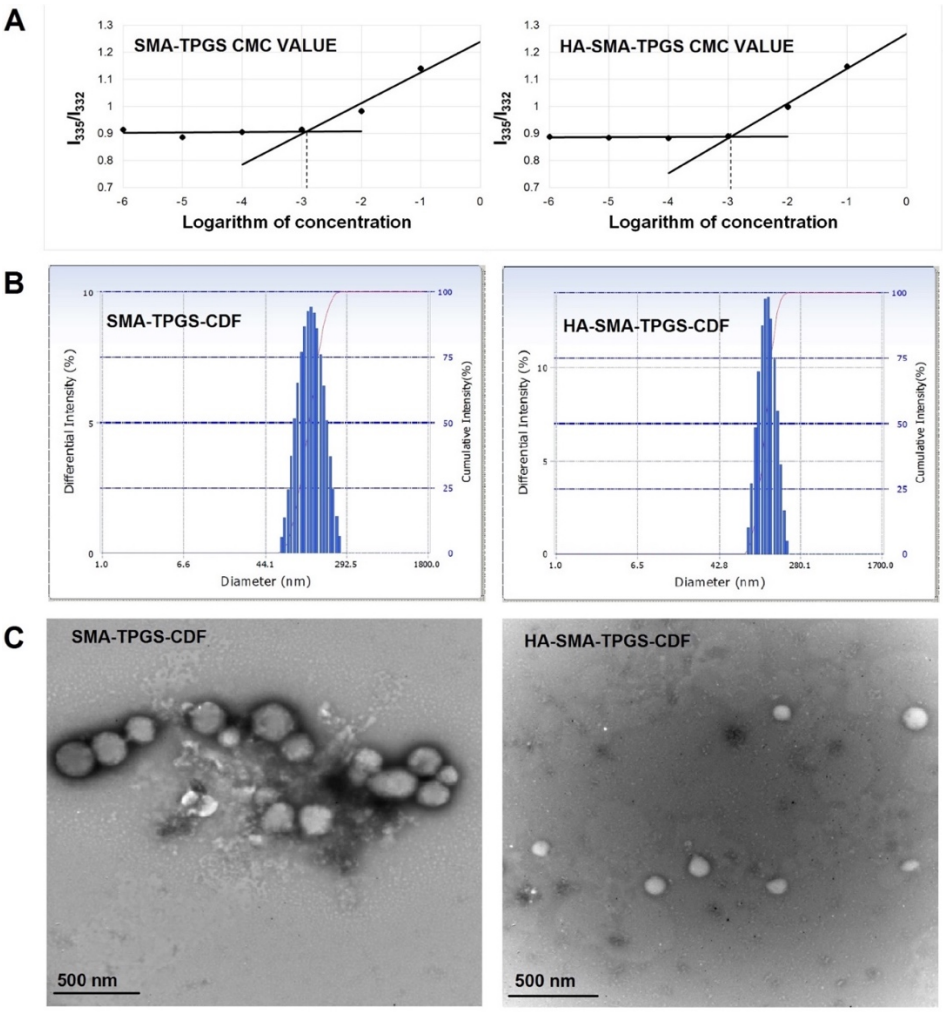

Figure 6. A) Plots of the fluorescence of excitation wavelengths ration of $I_{335\ nm}$/ $I_{332\ nm}$ from pyrene *vs.* the concentrations of SMA-TPGS and HA-SMA-TPGS in aqueous solution. (B) Hydrodynamic size of SMA-TPGS-CDF nanomicelles and HA-SMA-TPGS nanomicelles by DLS. (C) The morphology of SMA-TPGS-CDF nanomicelles and HA-SMA-TPGS nanomicelles characterized by TEM. Scale bar: 500 nm.

3.2.2 Characterization of CDF-loaded nanomicelles

The average particles size of TPGS-SMA-CDF showed a hydrodynamic size of 167.6 nm (PDI 0.087) and HA-TPGS-SMA-CDF showed a hydrodynamic size of 129.4 nm (PDI 0.118) (Figure 6B). The morphology of CDF-loaded nanomicelles was characterized by TEM (Figure 6C). The data revealed that the size of TPGS-SMA-CDF is around 150 – 180 nm and HA-TPGS-SMA-CDF is

around 120 – 150 nm. Both micelles were spherical in shape with a smooth surface. The particles size visualized by TEM were in agreement with the size acquired by DLS. The drug CDF encapsulation and loading were evaluated by HPLC method. The TPGS-SMA-CDF loading was14.9 ± 1.4% and encapsulation efficiency 84.3 ± 2.4%. The HA-TPGS-SMA-CDF loading was 19.6 ± 1.8% and the encapsulation efficiency 81.8 ± 3.7% (n=3) respectively.

3.2.3 *In vitro* release profile of CDF-loaded nanomicelles

As illustrated by figure 7, both SMA-TPGS-CDF nanomicelles and HA-SMA-TPGS-CDF nanomicelles showed practically identical fast release profiles at various pH conditions. The cumulative release of CDF for SMA-TPGS-CDF and HA-SMA-TPGS-CDF micelles in 24h, at pH 7.4 was found to be 67.56%±2.87, 78.65%±2.58. At pH 5.5 it was found to be 57.9%±6.95 and 69.53%±4.01. After 72h, the cumulative release of the CDF for SMA-TPGS-CDF and HA-SMA-TPGS-CDF micelles at physiological pH was 84.73%±7.4 and 86.97%±5.85. At lysosomal pH it was 77.98%±6.9 and 84.59%±6.35, respectively.

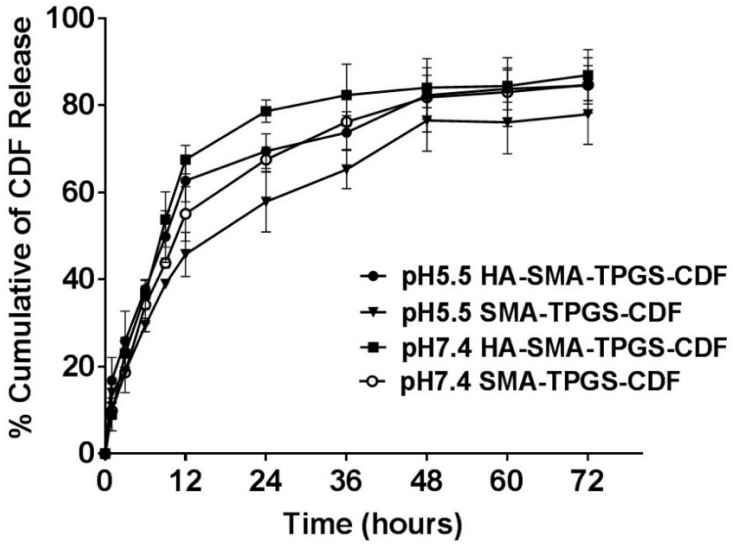

Figure 7. *In vitro* drug release study of SMA-TPGS-CDF nanomicelles and HA-SMA-TPGS-CDF nanomicelles incubated in PBS at pH 5.5 and 7.4, 37°C, respectively. Data are presented as mean ± SD, n=3.

3.2.4 Cellular uptake study

The fluorescence microscopic image (figure 8.) shows the different wavelength of fluorescence intensity in MDA-MB-231 and MDA-MB-468 cells. The blue-fluorescence indicated the signal of nuclei stained with Hoechst, and the red-fluorescent illustrated the signal of Rhodamine B. However, with both images presented in MDA-MB-231 and MDA-MB-468 cells, the targeted nanomicelles showed highest red-fluorescence intensity which corroborated with faster cellular uptake for the HA-targeted micelles than the non-targeted micelles and free Rhodamine B. Most probably reason for higher uptake of targeted nanomicelles was attributed to the HA affinity to CD44 receptor-mediated endocytosis on the surface of cells.

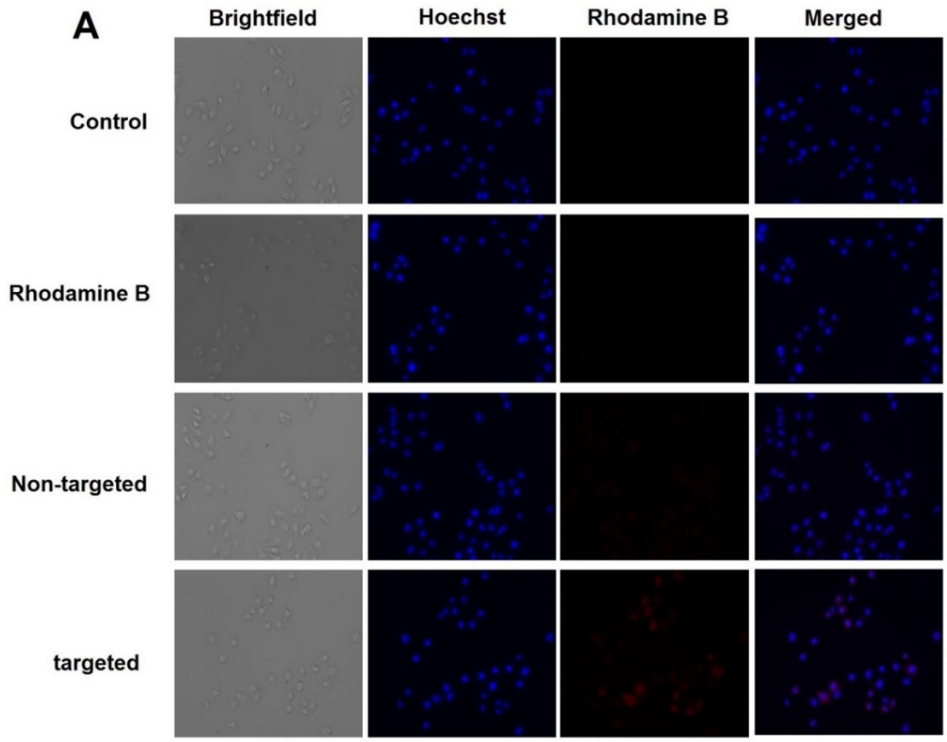

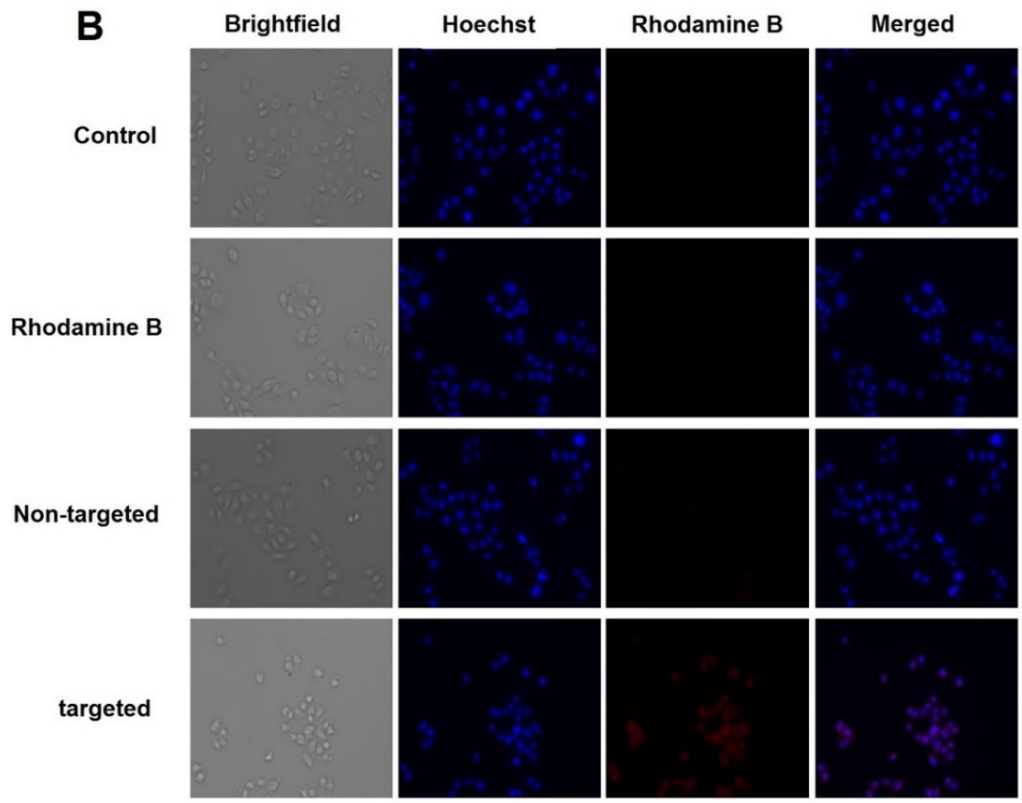

Figure 8. Fluorescence microscopic images of (A) MDA-MB-231, and (B) MDA-MB-468 cells after 3h incubation with Rhodamine B labeled nanomicelles and free Rhodamine B. Blue and red colors fluorescence light indicate cell nuclei and Rhodamine B, respectively.

3.2.5 *In vitro* Cytotoxicity Assay

The cell viability was determined by MTT assay which investigated the nanomicelle-cytotoxicity in figure 9. We used human triple negative breast cancer cell line, MDA-MB-231 and MDA-MB-468, to compare the cytotoxicity of free CDF, SMA-TPGS-CDF micelles and HA-TPGS-SMA-CDF micelles. HA-TPGS-SAM-CDF micelles showed a lower IC_{50} value compared to non-targeted micelles and free drug as shown in figure 9A. For MDA-MBA-231, in 24h and 48h the IC_{50} of free CDF was 280.4 nM and 161.8 nM. The IC_{50} of non-targeted micelles, SMA-TPGS-CDF micelles was 196.1 nM and 96.3 nM. The most affected one were the

targeted micelles, HA-SMA-TPGS-CDF micelles, the IC50 being 88.7 nM and 59.3 nM. A similar situation was observed in MDA-MB-468 cells, in 24h and 48h the IC_{50} of free CDF was 468.8 nM and 151.4 nM. The IC_{50} of non-targeted micelles, SMA-TPGS-CDF micelles, was 110.9 nM and 65.6 nM, and with the targeted micelles, HA-SMA-TPGS-CDF micelles, the IC50 was 99.1 nM and 59.9 nM. These results suggested that the higher cytotoxicity of targeted micelles could be attributed to the affinity of targeting ligand to CD44 receptor on the surface of cells.

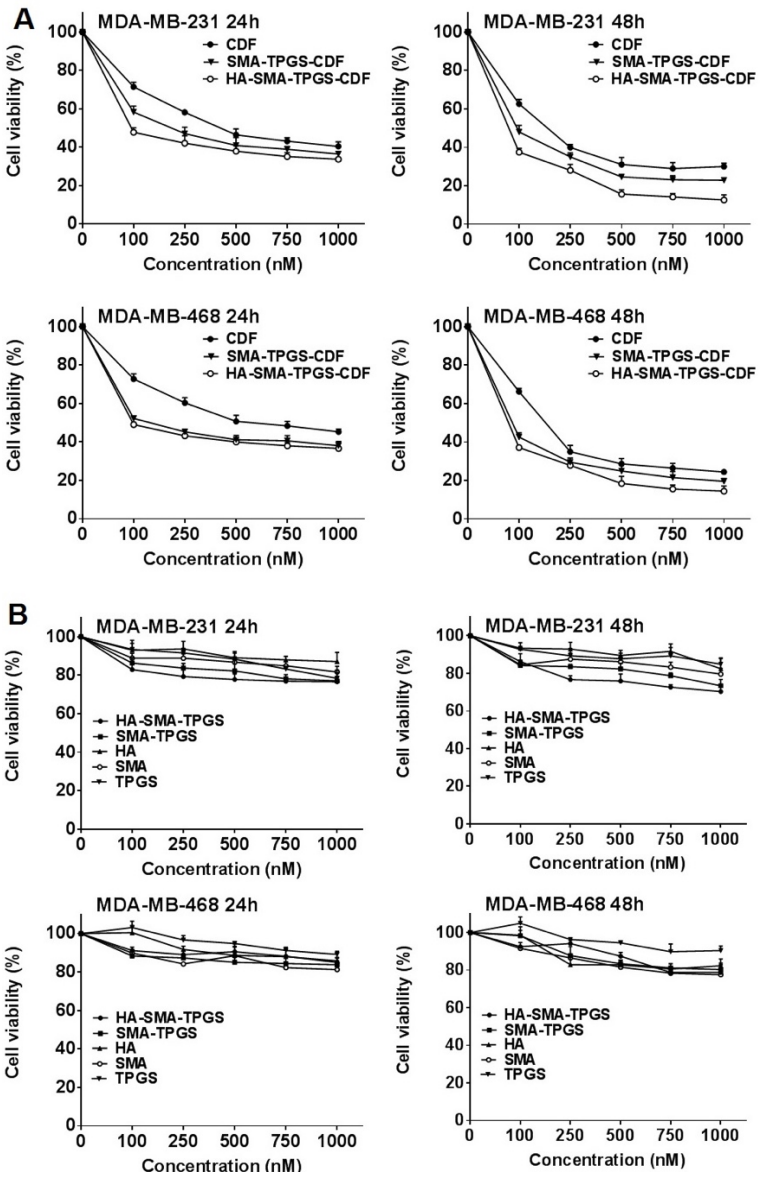

Figure 9. 24h and 48h viability assay on MDA-MB-231 and MDA-MB-468 treated with (A) Free CDF, SMA-TPGS-CDF nanomicelles and HA-SMA-TPGS-CDF nanomicelles at various total drug concentrations. (B) HA, SMA, TPGS, SMA-TPGS copolymer, SMA-TPGS copolymer at various total drug concentrations. Data represent mean ± SD, n=6.

3.2.6 CD44 receptor blocking assay

To further verify whether the uptake of the HA targeted CDF loaded micelles was due to CD44 receptor, the receptor blocking assay was studied (in figure 10.) by pre-treating the cells with an excess amount of HA (5 mg/ml) before formulation incubation. In MDA-MB-231 cells, it was observed that before CD44 receptor blockade, the IC_{50} value of 24h treatment free CDF, non-targeted micelles and targeted micelles were 280.4 nM, 196.1 nM, 88.7 nM. But after the receptor blockade, the IC_{50} value of free CDF and non-targeted micelles and targeted micelles were 279.3 nM, 200.2 nM, 194.2 nM. For 48h treatment the IC_{50} value of targeted micelles were changed from 59.3 nM to 94.2 nM. We could also observe the increasing shift in MDA-MB-468. The increasing IC_{50} value of targeted formulation indicated that the overexpression of CD44 receptor in cancer surface might be the primary pathway for targeted micelles to achieve active targeting.

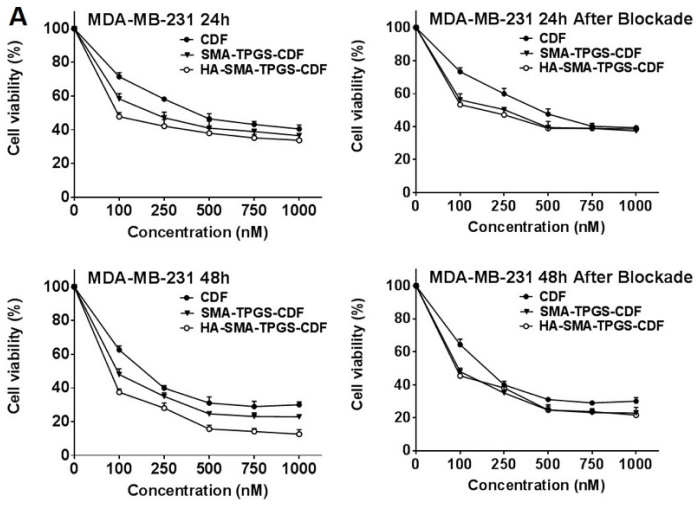

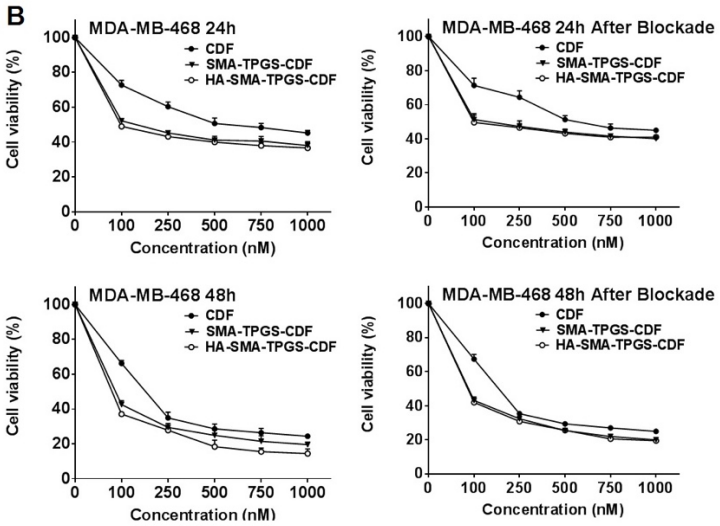

Figure 10. *In vitro* cytotoxicity assay observed at 24h and 48h after CD44 receptor blockade and treating of MDA-MB-231 and MDA-MB-468 with free CDF, SMA-TPGS-CDF nanomicelles and HA-SMA-TPGS-CDF nanomicelles at various total drug concentrations. Data represent mean ± SD, n=6.

3.2.7 Fluorescence activated cell sorting (FACS) analysis

Flow cytometry analysis is, as shown in figure 11, comparing free-CDF, SMA-TPGS conjugates, HA-SMA-TPGS conjugates, SMA-TPGS-CDF micelles, HA-SMA-TPGS-CDF micelles. As expected, targeted nanomicelles HA-SMA-TPGS-CDF induced more apoptosis in both MDA-MB-231 and MDA-MB-468 cells line. The ratio of double (Annexin V-FITC/PI) – positive cells in MDA-MBA-231 and MDA-MB-468 of each formulation (free-CDF, SMA-TPGS conjugate, HA-SMA-TPGS conjugate, SMA-TPGS-CDF micelles, HA-SMA-TPGS-CDF micelles) is shown in figure 11. Briefly, for MDA-MB-231 cells line, the early apoptosis and total apoptosis of free CDF, SMA-TPGS-CDF micelles, HA-SMA-TPGS-CDF micelles was 15.1%, 37.2%, 60.4% and 37.8%, 48.3%, 67.8%, respectively. For MDA-MB-468 cells line, the ratio was13.8%, 19.8%, 15.7% and 22.6%, 29.9%, 33.3%. These

results demonstrated that targeted formulation enhanced the CDF delivery and accumulation, which are mediated by the targeted ligand HA with CD44 receptor.

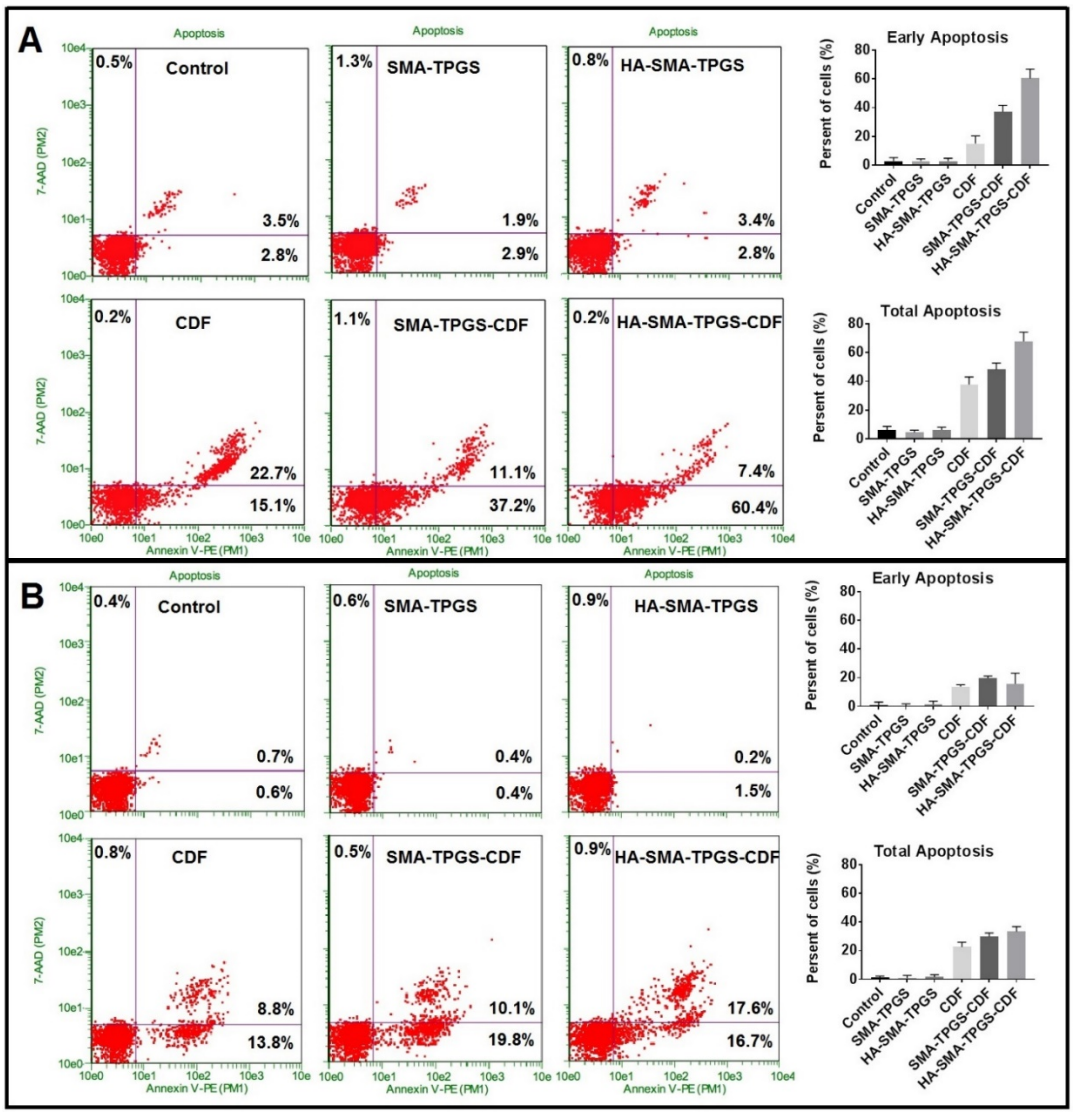

Figure 11. Free CDF, SMA-TPGS-CDF nanomicelles and HA-SMA-TPGS-CDF nanomicelles with an increasing apoptosis measured by FACs using staining of Annexin V-FITC-FITC and PI in (A) MDA-MB-231 and (B) MDA-MB-468. SMA-TPGS copolymer, SMA-TPGS copolymer set as control.

3.2.8 Western Blot

The previous study had identified that drug CDF can cause inactivation of carcinomas signaling pathways and down-regulation of NF-κB and up-regulation

of PTEN expression level. So, western blot was performed to detect the expression level of PTEN and NF-κB in protein level after treating with the formulation. In figure 12, in both MDA-MB-231 and MDA-MB-468 cells, it showed a significant down-regulation of NF- κB and up-regulation of PTEN in the treatment group. In detail, compared to free CDF, non-targeted micelles, and targeted micelles, PTEN level showed in MDA-MB-231, 1.94-fold, 2.52-fold and 3.3-fold upregulated compared to control respectively. Moreover, in MDA-MB-468, PTEN level displayed 1.54-fold, 2.47-fold and 2.52-fold upregulation compared to control. To determine NF-κB level the results showed in MDA-MB-231, 0.5-fold, 0.32-fold and 0.21-fold downregulated compared to control respectively. In MDA-MB-468, NF-κB level displayed 0.63-fold, 0.33-fold and 0.52-fold downregulation compared to control.

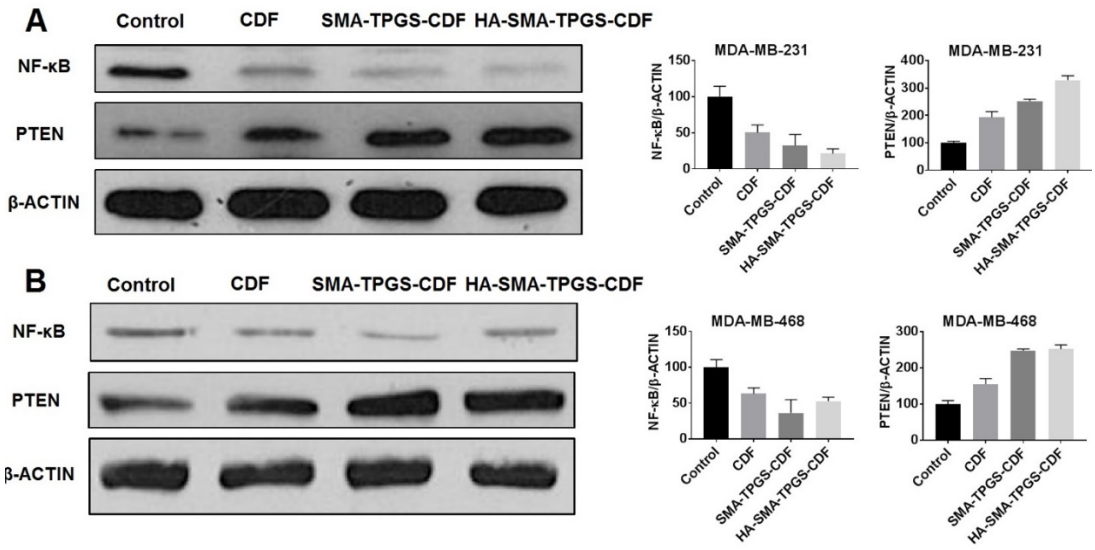

Figure 12. Western blot showing the expression downregulation of PTEN level and upregulation of NF-κB level in protein level after treating with the CDF, SMA-TPGS-CDF nanomicelles and HA-SMA-TPGS-CDF nanomicelles in (A) MDA-MB-231 and (B) MDA-MB-468 cells.

CHAPTER 4. DISCUSSION

4.1 Explore the pH-dependent redox activity in Cerium oxide nanoparticles for selective cancer cell killing

Elevated levels of reactive oxygen species can enhance oxidative stress in many diseases, including diabetes [94], cardiovascular disease[95], neurological disorders [96] and cancer[97]. ROS can be characterized as a potential carcinogen when elevated levels are found in intracellular environments leading to oxidative stress and even causing cells death due to the DNA and protein damage[98–100]. Redox-responsive cerium oxide nanoparticles can play a versatile role in cancer therapy due to their ability to induce oxidative stress only under tumorigenic low pH (~6.4 units) conditions while playing a tissue protective role under normal (7.4) pH conditions. Therefore, we developed polyethylene glycol polymer (PEG) and glycine (GLY)-coated cerium oxide nanoparticles to enhance their aqueous solubility. The size of cerium oxide nanoparticles was less than 20 nm. The cellular cytotoxicity results and quantification of intracellular levels of reactive oxygen species showed that cerium oxide nanoparticles in tumor cells were mediated by the pro-oxidant property of cerium oxide nanoparticles under relative low pH conditions (pH~6.5) of the tumor microenvironment whereas cerium oxide nanoparticles played a (cytoprotective) anti-oxidant role, scavenging reactive oxygen species (ROS) and reducing oxidative stress (under normal pH conditions or pH~7.4). The main reason of this bifunctional mode of action is because of the ability of pH-dependent redox activity in cerium oxide nanoparticles that can be exploited for selective cancer cell killing.

4.2 Hyaluronic acid engineered nanomicelles (HA-SMA-TPGS) for the targeted delivery of CDF to CD44 overexpressing cancer cells

The major issue of conventional chemotherapy using small molecule drug is indiscriminate distribution of the drug to tumor tissue leading to inadequate drug targeting that also causes toxicity to normal tissue. Most conventional anticancer agents are also highly hydrophobic and water insoluble. Based on our previous study, amphiphilic SMA was conjugated with targeting ligand to form a stable self-assembling micelles or nanoparticles to encapsulate chemotherapeutic drugs. The SMA micelles exhibited a high drug loading and encapsulation efficiency improving the solubility issue of anticancer compound. The results showed that the micelles could achieve passive targeting based on EPR effect and active targeting based on the high affinity of HA to CD44 receptor which is overexpressed in many cancer cells surface[34,93]. The SMA polymer conjugated with anticancer compound (SMANCS) has been approved for human clinical use[81,82]. However, multidrug resistant (MDR) in cancer is one of the main challenge for cancer therapy, after relapse of the disease. MDR is caused by several mechanisms including drug-efflux due to upregulation of P-glycoprotein. In this regard, it was found that vitamin E TPGS could reduce P-glycoprotein thus inhibiting the efflux pump. Moreover, TPGS is an amphiphilic compound which can enhance solubility, absorption, permeation and improve cellular uptake of chemotherapy agents[86,89,90,101]. For these advantages, we report herein, hyaluronic acid decorated styrene-maleic acid (SMA) copolymer with vitamin E TPGS nanomicelles for efficient drug delivery

to CD44 receptor overexpressing cancer including triple negative breast cancer, also addressing the poor aqueous solubility issue of anticancer compounds.

In our previous study, HA-SMA was synthesized and characterized to deliver anticancer compounds for pancreatic cancer[34]. In this study, we continued using HA and SMA as our carrier and conjugated with TPGS to develop a new drug delivery system which can improve the solubility of CDF and overcome multidrug resistant. The synthesis of HA-SMA-TPGS and SMA-TPGS carrier was confirmed by FTIR spectrum and ^{1}H NMR (Figure 4. and figure 5.). SMA anhydride ring had an opening reaction to conjugate with the alcohol groups on TPGS and HA to form the targeting carrier, HA-SMA-TPGS. For non-targeting carrier, no HA was used in this reaction. Then HA-SMA-TPGS-CDF and SMA-TPGS-CDF were prepared using our previous method[102,103]. Next, we tried different ratios of TPGS and HA to select the smallest size of nanomicelles when it is encapsulated with CDF. Finally, the hydrodynamic size of HA-SMA-TPGS-CDF was 129.4nm (PDI 0.118) and for the SMA-TPGS-CDF was 167.6nm (PDI 0.087). TEM image reconfirmed the size range of both targeted and non-targeted nanomicelles which was in good consistency with the hydrodynamic size. It has been widely reported that nano-range delivery system with the size less than 200nm was likely to achieve long blood circulation effect by hiding to reticuloendothelial system (RES) and increase distribution in tumor tissue through enhanced permeability and retention effect (EPR)[60,104]. Our results showed that all the targeted and non-targeted nanomicelles were in an ideal size range to achieve passive targeting EPR effect and avoiding recognition of RES.

To determine the self-assembled nanomicelles of HA-SMA-TPGS and SMA-TPGS carrier in aqueous media, critical micelles concentration (CMC) values were measured using fluorescence spectroscopy with pyrene as the probe. When the micelles were formed, when the concentration of HA-SMA-TPGS and SMA-TPGS increased, the fluorescence excitation spectra intensity lead to the peak absorbance wavelength shift from λ=332nm to λ=335nm. The CMC value calculated by plotting the I_{335nm}/I_{332nm} excitation intensity began to increase markedly versus the logarithm of the concentration of HA-SMA-TPGS and SMA-TPGS. The lower CMC value meant both HA-SMA-TPGS and SMA-TPGS were easy to form nanomicelles in lower carrierconcentration. Drug loading studies for both targeted and non-targeted micelles showed a high CDF loading. The reason why targeted micelles showed a higher CDF loading was because of the influence of HA chains on the surface of micelles that established interior hydrophobic cavities larger than the non-targeted micelles to encapsulate more drugs.

From the *in vitro* drug release profiles from targeted and non-targeted nanomicelles in different pH conditions, acid conditions pH 5.5 (endosomes of cancer cells) and normal conditions pH 7.4 (normal blood environment) were simulated. The result showed both HA-SMA-TPGS-CDF and SMA-TPGS-CDF presented a fast release rate at all conditions. Compared with normal pH (pH 7.4) and acidic pH (pH 5.) the CDF release rate was slower in acidic pH. One explanation for that could be polymer in protonated state, causing increased hydrophobicity of the micelles in media which performed a strong interaction with the hydrophobic drug, thus constraining CDF release[105]. Compared with

targeted and non-targeted micelles, HA-SMA-TPGS-CDF displayed a faster rate of drug release. The faster rate of CDF release may be explained by the influence of HA chains on the surface of micelles that led to steric stabilization endowed.

Having confirmed the ideal physical and chemical properties of HA-SMA-TPGS-CDF and SMA-TPGS-CDF nanomicelles. Next step, *in vitro* cellular uptake of micelles and intracellular distribution behaviors of Rhodamine B was detected by fluorescent microscopy in MDA-MB-231 and MDA-MB-468 cells. Both cells lines showed significant higher red fluorescence intensity in Rhodamine B labeled targeted formulation compared with the non-targeted formulation after 3h of incubation. The higher red fluorescence intensity indicated higher intracellular uptake capabilities. That results implied the targeted formulation, HA-SMA-TPGS, had a higher intracellular uptake than the non-targeted formulation, SMA-TPGS.

The cytotoxicity of CDF, SMA-TPGS-CDF micelles and HA-SMA-TPGS-CDF micelles was monitored using *in vitro* cytotoxicity assay on MDA-MB-231 and MDA-MB-468 cells. As shown in figure 9A. CDF and targeted, non-targeted micelles showed high anticancer activity in both cells, and the cytotoxicity of targeted micelles was significantly higher than the non-targeted micelles and free CDF. The results not only showed a dose-dependent cytotoxicity of both micelles formulations but also displayed a time-dependent cytotoxicity of two micellar formulations. For the MDA-MB-231 cells, the IC_{50} of targeted micelles was 1.98-fold and 3.16-fold smaller compared to non-targeted micelles and free CDF in 24h, and for 48h targeted micelles was 1.62-fold and 2.73-fold compared to non-targeted micelles and free CDF. For the MDA-MB-468 cells, the IC_{50} of HA-SMA-

TPGS-CDF micelles was lower by 1.2-fold and 4.73-fold compared to SMA-TPGS-CDF micelles and free CDF in 24h, and for 48h targeted micelles was 1.1-fold and 2.52-fold compared to non-targeted micelles and free CDF. The significant enhancement of anticancer activity of targeted micelles could be attributed to the HA affinity to CD44 receptor which overexpression the surface of cancer cells. The reason why the cytotoxicity of targeted micelles compared to non-targeted micelles is not significantly different in MDA-MB-468, most probably reason was the MDA-MB-231 CD44 receptor overexpressing type was $CD44^{+}/CD24^{-}$, but MDA-MB-468 overexpressing type was $CD44^{+}/CD24^{+}$[106,107]. The different type of CD44 receptor overexpressing type influenced the affinity of HA to CD44 receptor. The higher cytotoxicity of HA-SMA-TPGS-CDF micelles revealed that the targeted nanomicelles were more potent for delivery of CDF compared to non-targeted, free CDF and polymers control which maintained low cytotoxicity to cancer cells. Further, CD44 receptor blockade study was performed to confirm the higher cytotoxicity of targeted micelles was mediated by the affinity of HA to the CD44 receptor. In MDA-MB-231 cells, the increasing shift of IC_{50} value of 24h was from 88.7 nM to 194.2 nM. For 48h treatment the IC_{50} value of targeted micelles was changed from 59.3 nM to 94.2 nM. We could also observe the increasing shift in MDA-MB-468. An increasing IC_{50} of HA-SMA-TPGS-CDF micelles could be observed after blockade CD44 receptor. These results showed that the binding and internalization of targeted micelles to MDA-MB-231 and MDA-MB-468 could be competitively inhibited by the saturated amount of HA, which demonstrated that the CD44 receptor mediated the interaction of targeted formulation.

The apoptosis assay is shown in figure 11. The percentage of early and late apoptotic cells after treating with targeted micelles in both two cells lines was significantly increased. In MDA-MB-231, the percentage of early apoptosis, HA-SMA-TPGS-CDF micelles was 4-fold and 1.62-fold higher compared to free CDF and SMA-TPGS-CDF micelles. The percentage of total apoptosis, targeted formulation was 1.79-fold and 1.4-fold higher compared to free CDF and non-targeted micelles. In MDA-MB-468, the percentage of early apoptosis HA-SMA-TPGS-CDF micelles was 1.13-fold and 0.8-fold higher compared to free CDF and SMA-TPGS-CDF micelles. The percentage of total apoptosis, targeted formulation was 1.48-fold and 1.11-fold higher compared to free CDF and non-targeted micelles. It should be noted that with non-targeted micelles treated on MDA-MB-468 cells, the percentage of early apoptosis cells was higher than target micelles. The probable reason could be the different type of CD44 receptor on the surface of the cells. However, for the percentage of total injured cells, the highest treatment was still targeted micelles. The apoptosis results clearly indicated that HA-SMA-TPGS-CDF micelles (targeted micelles) were more effective inducing apoptosis compared with SMA-TPGS-CDF (non-targeted) and free drug.

Based on our previous research, CDF can cause inactivation of carcinomas signaling pathways consistent with miR-21 and down-regulation of controls transcription of DNA, NF-κB, and up-regulation of MiR-200 and phosphatase and tensin homolog (PTEN)[30–32]. So, western blot assays were performed on MDA-MB-231 and MDA-MB-468 to determine the protein level of NF-κB and PTEN after treating with free CDF, non-targeted formulation and targeted formulation. For the

protein level of PTEN, HA-SMA-TPGS-CDF showed a significant upregulated in both MDA-MB-231 and MDA-MB-468 compared to SMA-TPGS-CDF, free CDF and control. Moreover, for the protein NF-κB, targeted formulation displayed a significant downregulation in both two cells lines compared to non-targeted, free CDF and control. In these study for NF-κB level presented in MDA-MB-468, the non-targeted formulation exhibited more downregulation compared to the targeted formulation. The results could be explained again based on the different type of CD44 receptor on the surface of MDA-MB-468. Thus, the western blot results implied the targeted formulation could more upregulate PTEN and downregulate NF-κB, compared to the non-targeted, free drug and control, which could promote cancer death and tumor suppressor activity.

4.3. Summary and future direction

In this study, we developed polymer-coated cerium oxide nanoparticles to enhance the solubility using poly ethylene glycol (PEG) and glycine (GLY). Based on the pH-dependent cytotoxic profiles shown at low pH only towards tumor cells, cerium oxide nanoparticles and polymer-coated cerium oxide nanoparticles may provide a novel strategy for improving selective cancer cell killing. Regarding delivery of anticancer agents to tumor cells we have developed a new HA-SMA-TPGS conjugate that can form stable micelles with anticancer drugs. The HA-SMA-TPGS nanomicelles have been shown to be a promising carrier to enhance the solubility of CDR with stable small nano-size (less than 200 nm), spherical in shape with a smooth surface morphology. Low CMC value and high drug loading capacity were obtained using HA-SMA-TPGS micelles indicating its stability for *in*

vivo drug delivery. The cellular uptake, cytotoxicity, flow cytometry and western blot study confirmed that the targeted nanomicelles with a high affinity to CD44 receptor achieved more cytotoxicity to breast cancer cells. These results indicate that HA-SMA-TPGS conjugate is able to deliver CDF to treat CD44 positive human breast cancer cells. The CD44 receptor targeting approach can not only be applied to triple negative breast cancer but also to a number of cancer cells that overexpressed CD44 receptor including pancreatic and lungs cancers. In summary, HA-SMA-TPGS-CDF nanomicelles hold promising potential delivery approach for intracellular delivery of CDF for the treatment of CD44 overexpressing cancer and to overcome multidrug resistance to chemotherapy. Based on the promising results shown by the redox modulated cerium oxide nanoparticles and the cancer cells targeting ability of the nanomicelles formulation HA-SMA-TPGS-CDF, the future direction of this project is to explore the combination therapy of the two modalities to achieve synergy for more effective cancer therapy with reduced side effects.

REFERENCES:

[1] C. Facts, Cancer Facts and Figures, (2017). doi:10.1101/gad.1593107.

[2] A.F. Vitug, L.A. Newman, Complications in Breast Surgery, Surg. Clin. North Am. 87 (2007) 431–451. doi:10.1016/j.suc.2007.01.005.

[3] K.P. McGuire, A.A. Santillan, P. Kaur, T. Meade, J. Parbhoo, M. Mathias, C. Shamehdi, M. Davis, D. Ramos, C.E. Cox, Are Mastectomies on the Rise? A 13-Year Trend Analysis of the Selection of Mastectomy Versus Breast Conservation Therapy in 5865 Patients, Ann. Surg. Oncol. 16 (2009) 2682–2690. doi:10.1245/s10434-009-0635-x.

[4] L.A. Newman, S.E. Singletary, Overview of Adjuvant Systemic Therapy in Early Stage Breast Cancer, Surg. Clin. North Am. 87 (2007) 499–509. doi:10.1016/j.suc.2007.01.002.

[5] A.S. Coates, M. Colleoni, A. Goldhirsch, Is adjuvant chemotherapy useful for women with luminal a breast cancer?, J. Clin. Oncol. 30 (2012) 1260–1263. doi:10.1200/JCO.2011.37.7879.

[6] J.M. Gatell, P. D, J.K. Rockstroh, C. Katlama, P. Yeni, A. Lazzarin, B. Clotet, J. Zhao, J. Chen, D.M. Ryan, R.R. Rhodes, J.A. Killar, L.R. Gilde, K.M. Strohmaier, A.R. Meibohm, M.D. Miller, D.J. Hazuda, M.L. Nessly, M.J. Dinubile, R.D. Isaacs, B. Nguyen, H. Teppler, B. Study, New England Journal, October. (2008) 339–354. doi:10.1056/NEJMoa1411087.

[7] K.A. McKinney, W. Thompson, A practical guide to prescribing hormone replacement therapy., Drugs. 56 (1998) 49–57. doi:10.2165/00003495-199856010-00005.

[8] National Institutes of Health Consensus Development Panel, National Institutes of Health Consensus Development Conference statement: adjuvant therapy for breast cancer, November 1-3, 2000., J. Natl. Cancer Inst. Monogr. 20892 (2001) 5–15. http://www.ncbi.nlm.nih.gov/pubmed/11773285.

[9] A.C. Wolff, M.E. Hammond, D.G. Hicks, M. Dowsett, L.M. McShane, K.H. Allison, D.C. Allred, J.M. Bartlett, M. Bilous, P. Fitzgibbons, W. Hanna, R.B. Jenkins, P.B. Mangu, S. Paik, E.A. Perez, M.F. Press, P.A. Spears, G.H. Vance, G. Viale, D.F. Hayes, A.S. of C. Oncology, C. of A. Pathologists, Recommendations for human epidermal growth factor receptor 2 testing in breast cancer: American Society of Clinical Oncology/College of American Pathologists clinical practice guideline update. TL - 31, J. Clin. Oncol. 31 VN-r (2013) 3997–4013. doi:10.1200/JCO.2013.50.9984.

[10] S. Kümmel, J. Holtschmidt, S. Loibl, Surgical treatment of primary breast cancer in the neoadjuvant setting, Br. J. Surg. 101 (2014) 912–924. doi:10.1002/bjs.9545.

[11] J.S. de Bono, A. Ashworth, Translating cancer research into targeted therapeutics., Nature. 467 (2010) 543–549. doi:10.1038/nature09339.

[12] D. Luong, P. Kesharwani, B.A. Killinger, A. Moszczynska, F.H. Sarkar, S. Padhye, A.K. Rishi, A.K. Iyer, Solubility enhancement and targeted delivery of a potent anticancer flavonoid analogue to cancer cells using ligand decorated dendrimer nano-architectures, J. Colloid Interface Sci. 484 (2016) 33–43. doi:10.1016/j.jcis.2016.08.061.

[13] H. Jung, H. Mok, Mixed Micelles for Targeted and Efficient Doxorubicin Delivery to Multidrug-Resistant Breast Cancer Cells, Macromol. Biosci. 16 (2016) 748–758. doi:10.1002/mabi.201500381.

[14] G. Szakacs, J.K. Paterson, J.A. Ludwig, C. Booth-Genthe, M.M. Gottesman, G. Szakács, J.K. Paterson, J.A. Ludwig, C. Booth-Genthe, M.M. Gottesman, Targeting multidrug resistance in cancer, Nat. Rev. Drug Discov. 5 (2006) 219–234. doi:10.1038/nrd1984.

[15] F. Kievit, M. Zhang, Surface engineering of iron oxide nanoparticles for targeted cancer therapy, Acc. Chem. Res. 44 (2011) 853–862. doi:10.1021/ar2000277.Surface.

[16] P.X. Ma, Biomimetic materials for tissue engineering, Adv. Drug Deliv. Rev. 60 (2008) 184–198. doi:10.1016/j.addr.2007.08.041.

[17] A. Wicki, D. Witzigmann, V. Balasubramanian, J. Huwyler, Nanomedicine in cancer therapy: Challenges, opportunities, and clinical applications, J. Control. Release. 200 (2015) 138–157. doi:10.1016/j.jconrel.2014.12.030.

[18] D. Luong, S. Sau, P. Kesharwani, A.K. Iyer, Polyvalent Folate-Dendrimer-Coated Iron Oxide Theranostic Nanoparticles for Simultaneous Magnetic Resonance Imaging and Precise Cancer Cell Targeting, Biomacromolecules. (2017) acs.biomac.6b01885. doi:10.1021/acs.biomac.6b01885.

[19] R. Mo, T. Jiang, Z. Gu, Enhanced anticancer efficacy by ATP-mediated liposomal drug delivery, Angew. Chemie - Int. Ed. 53 (2014) 5815–5820. doi:10.1002/anie.201400268.

[20] D.K. Kim, Y. Zhang, W. Voit, K. V. Rao, M. Muhammed, Synthesis and characterization of surfactant-coated superparamagnetic monodispersed iron oxide nanoparticles, J. Magn. Magn. Mater. 225 (2001) 30–36. doi:10.1016/S0304-8853(00)01224-5.

[21] A.K. Gupta, M. Gupta, Synthesis and surface engineering of iron oxide nanoparticles for biomedical applications, Biomaterials. 26 (2005) 3995–4021. doi:10.1016/j.biomaterials.2004.10.012.

[22] D. Ling, T. Hyeon, Chemical design of biocompatible iron oxide nanoparticles for medical applications, Small. 9 (2013) 1450–1466. doi:10.1002/smll.201202111.

[23] M. Javed Akhtar, M. Ahamed, S. Kumar, M. Majeed Khan, J. Ahmad, S.A. Alrokayan, Zinc oxide nanoparticles selectively induce apoptosis in human cancer cells through reactive oxygen species, Int. J. Nanomedicine. 7 (2012) 845–857. doi:10.2147/IJN.S29129.

[24] K.M. Al-khamis, R.M. Mahfouz, A.A. Al-warthan, M.R.H. Siddiqui, Synthesis and characterization of gallium oxide nanoparticles, Arab. J. Chem. 2 (2009) 73–77. doi:10.1016/j.arabjc.2009.10.001.

[25] M.S. Lord, M. Jung, W.Y. Teoh, C. Gunawan, J.A. Vassie, R. Amal, J.M. Whitelock, Cellular uptake and reactive oxygen species modulation of cerium oxide nanoparticles in human monocyte cell line U937, Biomaterials. 33 (2012) 7915–7924. doi:10.1016/j.biomaterials.2012.07.024.

[26] M.S. Wason, J. Zhao, Cerium oxide nanoparticles: Potential applications for cancer and other diseases, Am. J. Transl. Res. 5 (2013) 126–131.

[27] A. Clark, A. Zhu, K. Sun, H.R. Petty, Cerium oxide and platinum nanoparticles protect cells from oxidant-mediated apoptosis, J. Nanoparticle Res. 13 (2011) 5547–5555. doi:10.1007/s11051-011-0544-3.

[28] A. Asati, S. Santra, C. Kaittanis, J.M. Perez, Surface-charge-dependent cell localization and cytotoxicity of cerium oxide nanoparticles, ACS Nano. 4 (2010)

5321–5331. doi:10.1021/nn100816s.

[29] S. Padhye, S. Banerjee, D. Chavan, S. Pandye, K.V. Swamy, S. Ali, J. Li, Q.P. Dou, F.H. Sarkar, Fluorocurcumins as cyclooxygenase-2 inhibitor: Molecular docking, pharmacokinetics and tissue distribution in mice, Pharm. Res. 26 (2009) 2438–2445. doi:10.1007/s11095-009-9955-6.

[30] B. Bao, S. Ali, D. Kong, S.H. Sarkar, Z. Wang, S. Banerjee, A. Aboukameel, S. Padhye, P.A. Philip, F.H. Sarkar, Anti-tumor activity of a novel compound-CDF is mediated by regulating miR-21, miR-200, and pten in pancreatic cancer, PLoS One. 6 (2011) 1–12. doi:10.1371/journal.pone.0017850.

[31] B. Bao, S. Ali, S. Banerjee, Z. Wang, F. Logna, A.S. Azmi, D. Kong, A. Ahmad, Y. Li, S. Padhye, F.H. Sarkar, Curcumin analogue CDF inhibits pancreatic tumor growth by switching on suppressor microRNAs and attenuating EZH2 expression, Cancer Res. 72 (2012) 335–345. doi:10.1158/0008-5472.CAN-11-2182.

[32] A. Vyas, P. Dandawate, S. Padhye, A. Ahmad, F. Sarkar, Perspectives on new synthetic curcumin analogs and their potential anticancer properties., Curr. Pharm. Des. 19 (2013) 2047–69. doi:10.1016/j.surg.2006.10.010.Use.

[33] S.K. Basak, A. Zinabadi, A.W. Wu, N. Venkatesan, V.M. Duarte, J.J. Kang, C.L. Dalgard, M. Srivastava, F.H. Sarkar, M.B. Wang, E.S. Srivatsan, Liposome encapsulated curcumin-difluorinated (CDF) inhibits the growth of cisplatin resistant head and neck cancer stem cells., Oncotarget. 6 (2015) 18504–18517. doi:10.18632/oncotarget.4181.

[34] P. Kesharwani, S. Banerjee, S. Padhye, F.H. Sarkar, A.K. Iyer, Hyaluronic Acid Engineered Nanomicelles Loaded with 3,4-Difluorobenzylidene Curcumin for Targeted Killing of CD44+ Stem-Like Pancreatic Cancer Cells, Biomacromolecules.

16 (2015) 3042–3053. doi:10.1021/acs.biomac.5b00941.

[35] P. Kesharwani, L. Xie, G. Mao, S. Padhye, A.K. Iyer, Hyaluronic acid-conjugated polyamidoamine dendrimers for targeted delivery of 3,4-difluorobenzylidene curcumin to CD44 overexpressing pancreatic cancer cells, Colloids Surfaces B Biointerfaces. 136 (2015) 413–423. doi:10.1016/j.colsurfb.2015.09.043.

[36] D. Luong, P. Kesharwani, R. Deshmukh, M.C.I. Mohd Amin, U. Gupta, K. Greish, A.K. Iyer, PEGylated PAMAM dendrimers: Enhancing efficacy and mitigating toxicity for effective anticancer drug and gene delivery, Acta Biomater. 43 (2016) 14–29. doi:10.1016/j.actbio.2016.07.015.

[37] K.A. Gawde, P. Kesharwani, S. Sau, F.H. Sarkar, S. Padhye, S.K. Kashaw, A.K. Iyer, Synthesis and characterization of folate decorated albumin bio-conjugate nanoparticles loaded with a synthetic curcumin difluorinated analogue, J. Colloid Interface Sci. 496 (2017) 290–299. doi:10.1016/j.jcis.2017.01.092.

[38] X. Zhang, Y. Huang, S. Li, Nanomicellar carriers for targeted delivery of anticancer agents, Ther Deliv. 5 (2014) 53–68. doi:10.1021/nn405701q\r10.4155/tde.13.135.

[39] R.R. Sawant, V.P. Torchilin, Multifunctionality of lipid-core micelles for drug delivery and tumour targeting, Mol. Membr. Biol. 27 (2010) 232–246. doi:10.3109/09687688.2010.516276.

[40] Y. Tian, S. Mao, Amphiphilic polymeric micelles as the nanocarrier for peroral delivery of poorly soluble anticancer drugs., Expert Opin. Drug Deliv. 9 (2012) 687–700. doi:10.1517/17425247.2012.681299.

[41] H. Xu, P. Yang, H. Ma, W. Yin, X. Wu, H. Wang, D. Xu, X. Zhang, Amphiphilic block copolymers-based mixed micelles for noninvasive drug delivery, Drug Deliv. 7544

(2016) 1–9. doi:10.3109/10717544.2016.1149743.

[42] A. Gothwal, I. Khan, U. Gupta, Polymeric Micelles: Recent Advancements in the Delivery of Anticancer Drugs, Pharm. Res. 33 (2016) 18–39. doi:10.1007/s11095-015-1784-1.

[43] M. Cagel, F.C. Tesan, E. Bernabeu, M.J. Salgueiro, M.B. Zubillaga, M.A. Moretton, D.A. Chiappetta, Polymeric mixed micelles as nanomedicines: Achievements and perspectives, Eur. J. Pharm. Biopharm. 113 (2017) 211–228. doi:10.1016/j.ejpb.2016.12.019.

[44] X. Guo, C. Shi, J. Wang, S. Di, S. Zhou, PH-triggered intracellular release from actively targeting polymer micelles, Biomaterials. 34 (2013) 4544–4554. doi:10.1016/j.biomaterials.2013.02.071.

[45] Y.Z. Du, L.L. Cai, J. Li, M.D. Zhao, F.Y. Chen, H. Yuan, F.Q. Hu, Receptor-mediated gene delivery by folic acid-modified stearic acid-grafted chitosan micelles., Int. J. Nanomedicine. 6 (2011) 1559–1568. doi:10.2147/IJN.S23828.

[46] M.S. Muthu, R.V. Kutty, Z. Luo, J. Xie, S.S. Feng, Theranostic vitamin E TPGS micelles of transferrin conjugation for targeted co-delivery of docetaxel and ultra bright gold nanoclusters, Biomaterials. 39 (2015) 234–248. doi:10.1016/j.biomaterials.2014.11.008.

[47] R.R. Sawant, A.M. Jhaveri, A. Koshkaryev, L. Zhu, F. Qureshi, V.P. Torchilin, Targeted transferrin-modified polymeric micelles: Enhanced efficacy in vitro and in vivo in ovarian carcinoma, Mol. Pharm. 11 (2014) 375–381. doi:10.1021/mp300633f.

[48] P. Zhang, L. Hu, Q. Yin, Z. Zhang, L. Feng, Y. Li, Transferrin-conjugated

polyphosphoester hybrid micelle loading paclitaxel for brain-targeting delivery: Synthesis, preparation and in vivo evaluation, J. Control. Release. 159 (2012) 429–434. doi:10.1016/j.jconrel.2012.01.031.

[49] T.Y. Kim, D.W. Kim, J.Y. Chung, S.G. Shin, S.C. Kim, D.S. Heo, N.K. Kim, Y.J. Bang, Phase I and pharmacokinetic study of Genexol-PM, a Cremophor-free, polymeric micelle-formulated paclitaxel, in patients with advanced malignancies, Clin. Cancer Res. 10 (2004) 3708–3716. doi:10.1158/1078-0432.CCR-03-0655.

[50] H.K. Ahn, M. Jung, S.J. Sym, D.B. Shin, S.M. Kang, S.Y. Kyung, J.W. Park, S.H. Jeong, E.K. Cho, A phase II trial of Cremorphor EL-free paclitaxel (Genexol-PM) and gemcitabine in patients with advanced non-small cell lung cancer, Cancer Chemother. Pharmacol. 74 (2014) 277–282. doi:10.1007/s00280-014-2498-5.

[51] T. Hamaguchi, K. Kato, H. Yasui, C. Morizane, M. Ikeda, H. Ueno, K. Muro, Y. Yamada, T. Okusaka, K. Shirao, Y. Shimada, H. Nakahama, Y. Matsumura, A phase I and pharmacokinetic study of NK105, a paclitaxel-incorporating micellar nanoparticle formulation., Br. J. Cancer. 97 (2007) 170–176. doi:10.1038/sj.bjc.6603855.

[52] K. Kato, K. Chin, T. Yoshikawa, K. Yamaguchi, Y. Tsuji, T. Esaki, K. Sakai, M. Kimura, T. Hamaguchi, Y. Shimada, Y. Matsumura, R. Ikeda, Phase II study of NK105, a paclitaxel-incorporating micellar nanoparticle, for previously treated advanced or recurrent gastric cancer, Invest. New Drugs. 30 (2012) 1621–1627. doi:10.1007/s10637-011-9709-2.

[53] S. Danson, D. Ferry, V. Alakhov, J. Margison, D. Kerr, D. Jowle, M. Brampton, G. Halbert, M. Ranson, Phase I dose escalation and pharmacokinetic study of pluronic polymer-bound doxorubicin (SP1049C) in patients with advanced cancer., Br. J.

Cancer. 90 (2004) 2085–2091. doi:10.1038/sj.bjc.6601856.

[54] J.W. Valle, A. Armstrong, C. Newman, V. Alakhov, G. Pietrzynski, J. Brewer, S. Campbell, P. Corrie, E.K. Rowinsky, M. Ranson, A phase 2 study of SP1049C, doxorubicin in P-glycoprotein-targeting pluronics, in patients with advanced adenocarcinoma of the esophagus and gastroesophageal junction, Invest. New Drugs. 29 (2011) 1029–1037. doi:10.1007/s10637-010-9399-1.

[55] Y. Lu, K. Park, Polymeric micelles and alternative nanonized delivery vehicles for poorly soluble drugs, Int. J. Pharm. 453 (2013) 198–214. doi:10.1016/j.ijpharm.2012.08.04.

[56] M.S. Lee, E.C. Dees, A.Z. Wang, Nanoparticle-Delivered Chemotherapy : Old Drugs in New Packages, (2017) 198–209.

[57] D.O. Scott, A. Ghosh, L. Di, T.S. Maurer, Passive drug permeation through membranes and cellular distribution, Pharmacol. Res. 117 (2017) 94–102. doi:10.1016/j.phrs.2016.11.028.

[58] J. Fang, H. Nakamura, H. Maeda, The EPR effect: Unique features of tumor blood vessels for drug delivery, factors involved, and limitations and augmentation of the effect, Adv. Drug Deliv. Rev. 63 (2011) 136–151. doi:10.1016/j.addr.2010.04.009.

[59] H. Maeda, T. Sawa, T. Konno, Mechanism of tumor-targeted delivery of macromolecular drugs, including the EPR effect in solid tumor and clinical overview of the prototype polymeric drug SMANCS, J. Control. Release. 74 (2001) 47–61. doi:10.1016/S0168-3659(01)00309-1.

[60] A.K. Iyer, G. Khaled, J. Fang, H. Maeda, Exploiting the enhanced permeability and retention effect for tumor targeting, Drug Discov. Today. 11 (2006) 812–818.

doi:10.1016/j.drudis.2006.07.005.

[61] H. Maeda, H. Nakamura, J. Fang, The EPR effect for macromolecular drug delivery to solid tumors: Improvement of tumor uptake, lowering of systemic toxicity, and distinct tumor imaging in vivo, Adv. Drug Deliv. Rev. 65 (2013) 71–79. doi:10.1016/j.addr.2012.10.002.

[62] J. Entwistle, C.L. Hall, E.A. Turley, HA receptors: Regulators of signalling to the cytoskeleton, J. Cell. Biochem. 61 (1996) 569–577. doi:10.1002/(SICI)1097-4644(19960616)61:4<569::AID-JCB10>3.0.CO;2-B.

[63] K.N. Sugahara, T. Hirata, H. Hayasaka, R. Stern, T. Murai, M. Miyasaka, Tumor cells enhance their own CD44 cleavage and motility by generating hyaluronan fragments, J. Biol. Chem. 281 (2006) 5861–5868. doi:10.1074/jbc.M506740200.

[64] D.C. West, I.N. Hampson, F. Arnold, S. Kumar, Angiogenesis induced by degradation products of hyaluronic acid., Science. 228 (1985) 1324–6. doi:10.1126/science.2408340.

[65] R. Tannishtha, S.J. Morrison, M.F. Clarke, I.L. Weissman, Stem cells, cancer, and cancer stem cells, Nature. 414 (2001) 105–111. doi:10.1007/978-1-60327-933-8.

[66] W.M. Lau, E. Teng, H.S. Chong, K.A.P. Lopez, A.Y.L. Tay, M. Salto-Tellez, A. Shabbir, J.B.Y. So, S.L. Chan, CD44v8-10 is a cancer-specific marker for gastric cancer stem cells, Cancer Res. 74 (2014) 2630–2641. doi:10.1158/0008-5472.CAN-13-2309.

[67] W. Hyung, H. Ko, J. Park, E. Lim, B.P. Sung, Y.J. Park, G.Y. Ho, S.S. Jin, S. Haam, Y.M. Huh, Novel hyaluronic acid (HA) coated drug carriers (HCDCs) for human breast cancer treatment, Biotechnol. Bioeng. 99 (2008) 442–454.

doi:10.1002/bit.21578.

[68] I. Morath, T.N. Hartmann, V. Orian-Rousseau, CD44: More than a mere stem cell marker, Int. J. Biochem. Cell Biol. 81 (2016) 166–173. doi:10.1016/j.biocel.2016.09.009.

[69] H. Lee, K. Lee, I.K. Kim, T.G. Park, Synthesis, characterization, and in vivo diagnostic applications of hyaluronic acid immobilized gold nanoprobes, Biomaterials. 29 (2008) 4709–4718. doi:10.1016/j.biomaterials.2008.08.038.

[70] X. Deng, M. Cao, J. Zhang, K. Hu, Z. Yin, Z. Zhou, X. Xiao, Y. Yang, W. Sheng, Y. Wu, Y. Zeng, Hyaluronic acid-chitosan nanoparticles for co-delivery of MiR-34a and doxorubicin in therapy against triple negative breast cancer, Biomaterials. 35 (2014) 4333–4344. doi:10.1016/j.biomaterials.2014.02.006.

[71] J. Li, M. Huo, J. Wang, J. Zhou, J.M. Mohammad, Y. Zhang, Q. Zhu, A.Y. Waddad, Q. Zhang, Redox-sensitive micelles self-assembled from amphiphilic hyaluronic acid-deoxycholic acid conjugates for targeted intracellular delivery of paclitaxel, Biomaterials. 33 (2012) 2310–2320. doi:10.1016/j.biomaterials.2011.11.022.

[72] P. Liu, Z. Li, M. Zhu, Y. Sun, Y. Li, H. Wang, Y. Duan, Preparation of EGFR monoclonal antibody conjugated nanoparticles and targeting to hepatocellular carcinoma, J. Mater. Sci. Mater. Med. 21 (2010) 551–556. doi:10.1007/s10856-009-3925-8.

[73] R. Costa, A.N. Shah, C.A. Santa-Maria, M.R. Cruz, D. Mahalingam, B.A. Carneiro, Y. Kwang Chae, M. Cristofanilli, W.J. Gradishar, F.J. Giles, Targeting Epidermal Growth Factor Receptor in Triple Negative Breast Cancer: New Discoveries and Practical Insights for Drug Development, Cancer Treat. Rev. 53 (2017) 111–119. doi:10.1016/j.ctrv.2016.12.010.

[74] M.L. Mcmaster, S.Y. Kristinsson, I. Turesson, M. Bjorkholm, O. Landgren, NIH Public Access, Clin. Lymphoma. 9 (2010) 19–22. doi:10.3816/CLM.2009.n.003.Novel.

[75] H. Kuang, S.H. Ku, E. Kokkoli, The design of peptide-amphiphiles as functional ligands for liposomal anticancer drug and gene delivery, Adv. Drug Deliv. Rev. (2016). doi:10.1016/j.addr.2016.08.005.

[76] K.C. Brown, Peptidic tumor targeting agents: the road from phage display peptide selections to clinical applications., Curr. Pharm. Des. 16 (2010) 1040–54. doi:10.2174/138161210790963788.

[77] J. Wang, W. Liu, Q. Tu, J. Wang, N. Song, Y. Zhang, N. Nie, J. Wang, Folate-decorated hybrid polymeric nanoparticles for chemically and physically combined paclitaxel loading and targeted delivery, Biomacromolecules. 12 (2011) 228–234. doi:10.1021/bm101206g.

[78] X. Yang, A.K. Iyer, A. Singh, E. Choy, F.J. Hornicek, M.M. Amiji, Z. Duan, MDR1 siRNA loaded hyaluronic acid-based CD44 targeted nanoparticle systems circumvent paclitaxel resistance in ovarian cancer, Sci Rep. 5 (2015) 8509. doi:10.1038/srep08509.

[79] C. Zhao, X. Liu, J. Liu, Z. Yang, X. Rong, M. Li, X. Liang, Y. Wu, Transferrin conjugated poly (??-glutamic acid-maleimide-co-l-lactide)-1,2-dipalmitoylsn-glycero-3-phosphoethanolamine copolymer nanoparticles for targeting drug delivery, Colloids Surfaces B Biointerfaces. 123 (2014) 787–796. doi:10.1016/j.colsurfb.2014.10.024.

[80] M.L. Manca, I. Castangia, M. Zaru, A. Nácher, D. Valenti, X. Fernàndez-Busquets, A.M. Fadda, M. Manconi, Development of curcumin loaded sodium hyaluronate

immobilized vesicles (hyalurosomes) and their potential on skin inflammation and wound restoring, Biomaterials. 71 (2015) 100–109. doi:10.1016/j.biomaterials.2015.08.034.

[81] L.W. Seymour, S.P. Olliff, C.J. Poole, P.G. De Takats, R. Orme, D.R. Ferry, H. Maeda, T. Konno, D.J. Kerr, A novel dosage approach for evaluation of SMANCS [poly-(styrene-co-maleyl-half-n-butylate) - neocarzinostatin] in the treatment of primary hepatocellular carcinoma., Int. J. Oncol. 12 (1998) 1217–23.

[82] H. Maeda, SMANCS and polymer-conjugated macromolecular drugs: Advantages in cancer chemotherapy, Adv. Drug Deliv. Rev. 46 (2001) 169–185. doi:10.1016/S0169-409X(00)00134-4.

[83] P.P. Constantinides, J. Han, S.S. Davis, Advances in the use of tocols as drug delivery vehicles, Pharm. Res. 23 (2006) 243–255. doi:10.1007/s11095-005-9262-9.

[84] M.V.S. Varma, R. Panchagnula, Enhanced oral paclitaxel absorption with vitamin E-TPGS: Effect on solubility and permeability in vitro, in situ and in vivo, Eur. J. Pharm. Sci. 25 (2005) 445–453. doi:10.1016/j.ejps.2005.04.003.

[85] X. Li, P. Li, Y. Zhang, Y. Zhou, X. Chen, Y. Huang, Y. Liu, Novel mixed polymeric micelles for enhancing delivery of anticancer drug and overcoming multidrug resistance in tumor cell lines simultaneously, Pharm. Res. 27 (2010) 1498–1511. doi:10.1007/s11095-010-0147-1.

[86] J.A. Hyatt, K.J. Edgar, U.F. Schaefer, Mechanism of Inhibition of P-Glycoprotein Mediated Efflux by Vitamin E TPGS: Influence on ATPase Activity and Membrane Fluidity, 4 (2007) 465–474.

[87] E. Collnot, C. Baldes, U.F. Schaefer, K.J. Edgar, M.F. Wempe, C. Lehr, V. Tech, articles Vitamin E TPGS P-Glycoprotein Inhibition Mechanism : Influence on Conformational Flexibility , Intracellular ATP Levels , and Role of Time and Site of Access, 84 (2010) 423–429.

[88] P. Agrawal, Sonali, R.P. Singh, G. Sharma, A.K. Mehata, S. Singh, C. V. Rajesh, B.L. Pandey, B. Koch, M.S. Muthu, Bioadhesive micelles of d-α-tocopherol polyethylene glycol succinate 1000: Synergism of chitosan and transferrin in targeted drug delivery, Colloids Surfaces B Biointerfaces. 152 (2017) 277–288. doi:10.1016/j.colsurfb.2017.01.021.

[89] Z. Zhang, S. Tan, S.S. Feng, Vitamin E TPGS as a molecular biomaterial for drug delivery, Biomaterials. 33 (2012) 4889–4906. doi:10.1016/j.biomaterials.2012.03.046.

[90] Y. Guo, J. Luo, S. Tan, B.O. Otieno, Z. Zhang, The applications of Vitamin e TPGS in drug delivery, Eur. J. Pharm. Sci. 49 (2013) 175–186. doi:10.1016/j.ejps.2013.02.006.

[91] K. Greish, T. Sawa, J. Fang, T. Akaike, H. Maeda, SMA-doxorubicin, a new polymeric micellar drug for effective targeting to solid tumours, J. Control. Release. 97 (2004) 219–230. doi:10.1016/j.jconrel.2004.03.027.

[92] K. Tsukigawa, L. Liao, H. Nakamura, J. Fang, K. Greish, M. Otagiri, H. Maeda, Synthesis and therapeutic effect of styrene-maleic acid copolymer-conjugated pirarubicin, Cancer Sci. 106 (2015) 270–278. doi:10.1111/cas.12592.

[93] P. Kesharwani, S. Banerjee, S. Padhye, F.H. Sarkar, A.K. Iyer, Parenterally administrable nano-micelles of 3,4-difluorobenzylidene curcumin for treating pancreatic cancer, Colloids Surfaces B Biointerfaces. 132 (2015) 138–145.

doi:10.1016/j.colsurfb.2015.05.007.

[94] H. Kaneto, N. Katakami, M. Matsuhisa, T. Matsuoka, Role of reactive oxygen species in the progression of type 2 diabetes and atherosclerosis., Mediators Inflamm. 2010 (2010) 453892. doi:10.1155/2010/453892.

[95] K. Sugamura, J.F. Keaney, Reactive oxygen species in cardiovascular disease, Free Radic. Biol. Med. 51 (2011) 978–992. doi:10.1016/j.freeradbiomed.2011.05.004.

[96] K. Hensley, K. a Robinson, S.P. Gabbita, S. Salsman, R. a Floyd, Reactive oxygen species, cell signaling, and cell injury, Free Radic. Biol. Med. 28 (2000) 1456–1462. doi:10.1016/S0891-5849(00)00252-5.

[97] P. Schumacker, Reactive Oxygen Species in Cancer: A Dance with the Devil, Cancer Cell. 27 (2015) 156–157. doi:10.1016/j.ccell.2015.01.007.

[98] A.A. Alfadda, R.M. Sallam, Reactive oxygen species in health and disease., J. Biomed. Biotechnol. 2012 (2012) 936486. doi:10.1155/2012/936486.

[99] K. Datta, S. Sinha, P. Chattopadhyay, Reactive oxygen species in health and disease, Natl. Med. J. India. 13 (2000) 304–310. doi:10.1155/2012/936486.

[100] G.-Y. Liou, P. Storz, Reactive oxygen species in cancer., Free Radic. Res. 44 (2010) 479–96. doi:10.3109/10715761003667554.

[101] N. Duhem, F. Danhier, V. Préat, Vitamin E-based nanomedicines for anti-cancer drug delivery, J. Control. Release. 182 (2014) 33–44. doi:10.1016/j.jconrel.2014.03.009.

[102] A.K. Iyer, K. Greish, T. Seki, S. Okazaki, J. Fang, K. Takeshita, H. Maeda, Polymeric micelles of zinc protoporphyrin for tumor targeted delivery based on EPR

effect and singlet oxygen generation., J. Drug Target. 15 (2007) 496–506. doi:10.1080/10611860701498252.

[103] J. Fang, A.K. Iyer, T. Seki, H. Nakamura, K. Greish, H. Maeda, SMA-copolymer conjugate of AHPP: A polymeric inhibitor of xanthine oxidase with potential antihypertensive effect, J. Control. Release. 135 (2009) 211–217. doi:10.1016/j.jconrel.2009.01.006.

[104] H. Maeda, Macromolecular therapeutics in cancer treatment: The EPR effect and beyond, J. Control. Release. 164 (2012) 138–144. doi:10.1016/j.jconrel.2012.04.038.

[105] R. Stern, M.J. Jedrzejas, Hyaluronidases: Their genomics, structures, and mechanisms of action, Chem. Rev. 106 (2006) 818–839. doi:10.1021/cr050247k.

[106] M.O. Idowu, M. Kmieciak, C. Dumur, R.S. Burton, M.M. Grimes, C.N. Powers, M.H. Manjili, CD44(+)/CD24(-/low) cancer stem/progenitor cells are more abundant in triple-negative invasive breast carcinoma phenotype and are associated with poor outcome., Hum. Pathol. 43 (2012) 364–73. doi:10.1016/j.humpath.2011.05.005.

[107] C. Sheridan, H. Kishimoto, R.K. Fuchs, S. Mehrotra, P. Bhat-Nakshatri, C.H. Turner, R. Goulet, S. Badve, H. Nakshatri, CD44+/CD24- breast cancer cells exhibit enhanced invasive properties: an early step necessary for metastasis., Breast Cancer Res. 8 (2006) 59. doi:10.1186/bcr1610.

ABSTRACT

REDOX RESPONSIVE CERIUM OXIDE NANOPARTICLES AND CD44 TARGETED NANOMICELLES FOR SELECTIVE CANCER THERAPY

by

ZHAOXIAN WANG

May 2017

Advisor: Dr. Arun Iyer

Major: Pharmaceutical Sciences

Degree: Master of Science

Redox-responsive cerium oxide nanoparticles (CNPs) can play a versatile role in cancer therapy due to their ability to induce oxidative stress under proper pH conditions. Hyaluronic acid micelles with a high affinity to CD44 receptor which achieved more cytotoxicity towards cancer cells. The polymer-coated CNPs and HA-SMA-TPGS-CDF nanomicelles were developed for cancer therapy. The results showed that the toxicity of CNPs in tumor cells was mediated by the pro-oxidant property of CNPs under relative low pH conditions (pH~6.5) of the tumor microenvironment whereas CNPs play a (cytoprotective) anti-oxidant role, scavenging reactive oxygen species and reducing oxidative stress under normal pH conditions or pH~7.4. HA-SMA-TPGS-CDF nanomicelles held promising effective and potentially deliver approach to for intracellular delivery of 3,4-difluorobenzylidene diferuloylmethane due to higher accumulation and more cytotoxicity in cancers. Next, we will fabricate a combined nanodelivery structure

having cerium oxide nanoparticles and HA-SMA-TPGS copolymer for the treatment of cancers, warranting further investigations.

AUTOBIOGRAPHICAL STATEMENT

PRESENTATIONS

- ‘‘Redox Responsive Cerium Oxide Nanoparticles for Lung Cancer Therapy’’, Graduate Student Research Day, Wayne State University, Detroit, Michigan, October 7th, 2016
- ‘‘Redox Responsive Cerium Oxide Nanoparticles for Lung Cancer Therapy’’, Annual Research Forum, Wayne State University, Detroit, Michigan, October 5th, 2016